Asem *et al. BMC Genomics* (2025) 26:228
https://doi.org/10.1186/s12864-025-11391-6

BMC Genomics

RESEARCH

Open Access

Mitogenomic phylogeny and divergence time estimation of *Artemia* Leach, 1819 (Branchiopoda: Anostraca) with emphasis on parthenogenetic lineages

Alireza Asem[1*†], Chaojie Yang[1†], Stephanie De Vos[2†], Farnaz Mahmoudi[1], Lidong Xia[3], Chun-Yang Shen[4], Francisco Hontoria[5*], D. Christopher Rogers[6*] and Gonzalo Gajardo[7*]

Abstract

The brine shrimp *Artemia,* a crustacean adapted to the extreme conditions of hypersaline environments, comprises nine regionally distributed sexual species scattered (island-like) over heterogeneous environments and asexual (parthenogenetic) lineages with different ploidies. Such sexual and asexual interaction within the genus raises questions regarding the origin and time of divergence of both sexual species and asexual lineages, including the persistence of the latter over time, a problem not yet clarified using single mitochondrial and nuclear markers. Based on the complete mitochondrial genome of all species and parthenogenetic lineages, this article first describes the mitogenomic characteristics (nucleotide compositions, genome mapping, codon usage, and tRNA secondary structure) of sexual species and asexual types and, secondly, it provides a comprehensive updated phylogenetic analysis. Molecular dating and geographical evidence suggest that the ancestral *Artemia* taxon originated in *ca*. 33.97 Mya during the Paleogene Period. The mitogenomic comparisons suggest that the common ancestor of diploid and triploid parthenogenetic lineages (*ca*. 0.07 Mya) originated from a historical ancestor (*ca.* 0.61 Mya) in the Late Pleistocene. Additionally, the common ancestor of tetraploid and pentaploid parthenogenetic lineages (*ca.* 0.05 Mya) diverged from a historical maternal ancestor with *A. sinica* (*ca*. 0.96 Mya) in the early Pleistocene. The parthenogenetic lineages do not share a direct ancestor with any sexual species. The Asian clade ancestor diverged more recently (*ca.* 14.27 Mya, Middle Miocene). The mitogenomic characteristics, maternal phylogenetic tree, and especially divergence time prove that *A. monica* and *A. franciscana* are two biological species.

†Alireza Asem, Chaojie Yang, Stephanie De Vos contributed equally to this work as first author.

*Correspondence:
Alireza Asem
asem.alireza@gmail.com
Francisco Hontoria
hontoria@iats.csic.es
D. Christopher Rogers
Branchiopod@gmail.com
Gonzalo Gajardo
ggajardo@ulagos.cl
Full list of author information is available at the end of the article

Keywords Brine shrimp, Common ancestor, Evolutionary origin, Long branch length, Long branch attraction (LBA), MtDNA

Introduction

Artemia Leach, 1819 is a genus of halophilic zooplanktonic crustaceans commonly known as "brine shrimp", which are distributed in isolated hypersaline habitats across the world [1] with an island biogeography dispersal model [2–5]. *Artemia* is highly plastic across morphometric and morphological traits in both natural and laboratory conditions [6–11] and tends to exhibit accelerated molecular evolution very likely due to the mutagenic effect associated with ionic strength variance [12] and other stringent ecological conditions [13], combined with natural population expansion and contraction cycles. Additionally, natural salt lake ionic compositions, temperatures, and salinity heterogeneity, further affected by climatic changes and human perturbations [14, 15], have left mitogenomic signatures in *Artemia* bisexual species [1], which are also reflected in private mitochondrial haplotypes [4, 5, 16–23]. There is no classic "identification key" for the genus *Artemia* and taxonomic delimitation of sexual species and parthenogenetic lineages has been limited to reproductive mode [4, 24], geographical distribution [25, 26], and molecular markers [4, 5, 18, 21, 27].

Artemia consists of nine sexual species and four obligate parthenogenetic lineages [4, 23], regionally distributed around the world (except Antarctica) in arid and semiarid areas. Three species in the New World: *A. monica* Verrill, 1869 (Mono Lake, USA), *A. franciscana* Kellogg, 1906, (North, Central and South America, but introduced for commercial aquaculture in Eurasia, Africa and Australia), and *Artemia persimilis* Piccinelli and Prosdocimi, 1968, (Chile and Argentina). Six species in the Old World: *A. salina* (Linnaeus, 1758) (Europe and Africa); *A. urmiana* Günther, 1899 (Lake Urmia, Iran and the Crimean Peninsula); *A. sinica* Cai, 1989 (China); *A. amati* Asem, Eimanifar, Hontoria, Rogers and Gajardo, 2023 (Kazakhstan); *A. tibetiana* Abatzopoulos, Zhang and Sorgeloos 1998; and *A. sorgeloosi* Asem, Eimanifar, Hontoria, Rogers and Gajardo, 2023, the last two from the Tibetan Plateau. Obligate parthenogenetic *Artemia* consists of four lineages with different ploidy levels (di-, tri-, tetra- and pentaploid), all occurring in the Old World [18, 19, 21, 25, 28–38] and Australia [39–41].

Artemia evolutionary relationships have been studied with different tools, with some concordances and differences, from electrophoresis-based enzyme assays [42], morphometrical characteristics [4, 25, 26, 30, 32, 43–45], sequences of partial mitochondrial genes (*COI*, *16S* and *12S*) [4, 5, 17–19, 21, 27, 34, 38, 45], as well as the complete sequence of the nuclear *ITS1* gene [4, 21, 38, 46, 47], to nuclear simple sequence repeats (SSR) markers [4, 48, 49].

Triantaphyllidis et al. [43] argued that *A. urmiana* was significantly isolated from the other Asian groups based on morphometric characters. However, the use of mitochondrial markers demonstrates that Asian species have a common ancestor [4, 18, 38]. Baxevanis et al. [45] found that the Asian *A. tibetiana* and *A. urmiana* are genetically close taxa while morphometrically dissimilar. In contrast, South American *A. persimilis* and *A. urmiana* are significantly different genetically, while having similar morphometric patterns [45, 50]. Asem et al. [4] demonstrated no conformity between mitochondrial marker results and morphometric patterns. Examples of such inconsistencies follow.

The Mediterranean *A. salina* and *A. franciscana* group together based on mitochondrial *16S* rDNA RFLP analyses [45]. In the mitochondrial COI-based study of Muñoz et al., *A. salina* and *A. persimilis* were placed in the same clade, and *A. sinica* as a sister clade of *A. franciscana* and other Asian *Artemia*, with *A. franciscana* in between [16]. Maniatsi et al. using nuclear *ITS1* and mitochondrial *COI*, reported the American *A. franciscana* was sister to the Asian species and parthenogenetic lineages, and that *A. persimilis* was basal to both [18]. Using *COI* sequences, Eimanifar et al. found *A. salina* to be basal [21].

Overall, these studies show that *Artemia* maternal phylogenetic relationships are still unclear. Moreover, recent studies show that phylogenetic reconstructions based on short mitochondrial marker sequences do not necessarily reproduce the tree topologies and divergence estimates found using the complete mitogenome, which has increasingly become the marker of choice [51, 52].

Here, we use the complete mitochondrial genome (henceforth mitogenome) to refine *Artemia* phylogeny and divergence times and resolve the different results produced by the various studies on *Artemia* species and parthenogenetic lineages.

The mitogenome represents specific maternal origins and involves rapid evolutionary alterations without recombination [5, 53–59]. Additionally, mitochondria are responsible for ATP production, which is necessary to respond to critical environmental conditions such as high salinity and related hypoxia, demanding major oxygen consumption. The mitochondria regulate the expression of multiple genes in response to those and other environmental conditions [60]. The coordinated functioning of the whole mitochondrial complement is required for local adaptation. We used the *Artemia* mitogenome to (1) clarify *Artemia* phylogeny, (2) reconsider parthenogenetic lineage origins hypotheses, and (3) estimate divergence times and evolutionary ages of *Artemia* members. We also studied nucleotide compositions, genome mapping, codon usage, and tRNA secondary structure. A comprehensive updated phylogenetic study considering all species (some recently described) and parthenogenetic lineages is necessary to comprehend *Artemia's* evolutionary history, origin, and divergence.

Materials and methods

Sampling

Nine *Artemia* species and four parthenogenetic lineages were studied from topotype material, except *A. salina*, which has disappeared from its type locality (Lymington, England), and *A. persimilis* (Salinas Grandes de Hidalgo, Argentina), which was unavailable. We did not have access to the samples of "diploid parthenogenetic *Artemia* with *A. urmiana* type mitochondria (see Discussion). Further information of species and parthenogenetic lineages is summarized in Table 1.

Eggs from each locality were cultured following Hontoria and Amat [25], except *A. monica*, which was unhatchable; *A. monica* was sequenced directly from eggs (for more information, see DNA Extraction and Sequencing section). Only females were sequenced after reproduction mode confirmation by individual culture [4, 61], as in most Old-World populations, *Artemia* species and parthenogenetic lineages may coexist, and diploid parthenogens may produce rare males (see [62]). Ploidy levels were determined by karyotyping using cloned nauplii [38]. Taxonomic status of all sexual species were re-confirmed by applying NCBI's BLAST online platform (https://blast.ncbi.nlm.nih.gov), using *COI* sequences datasets [63], to confirm *Artemia* bisexual species identities, as the exotic American *A. franciscana* has been widely introduced in many countries all over the world.

DNA extraction and sequencing

Total genomic DNA was extracted individually from two adult females of each species and each parthenogenetic lineage, using the Rapid Animal Genomic DNA Isolation Kit (Sangon Biotech Co., Ltd., Shanghai, China; NO. B518221). In the case of *A. monica*, two individual decapsulated eggs were used for DNA extraction. Total genomic DNA was amplified following MALBAC Single Cell Whole Genome Amplification Kit no. KT110700150 (Yikon Genomics Co., Ltd. Jiangsu, CN). The Microvolume Spectrophotometer (MaestroGen Inc., Hsinchu, Taiwan) was utilized to check the quantity of amplified DNA. From each individual 600 ng of the amplified DNA was pooled and employed to build a single paired end (2×150 bp) genomic library using the NEBNext® UltraTM II DNA Library Prep Kit for Illumina (New England Biolabs, Ipswich, MA, USA) [4, 64]. Next-generation sequencing (>10 Gb) of the pooled DNA library was performed on one sequencing flow cell of a NovaSeq 6000 Illumina machine (Novogene Co., Tianjin, China).

Table 1 List of studied *Artemia* species and parthenogenetic lineages, their provenance and egg bank accession

Taxon status	Locality	Coordinates	Abb	Egg bank accession
A. salina	Sfax, Tunisia	34°43′N 10°45′E	SAL	ARC[a], Belgium
A. sinica	Yuncheng Lake, China	34°59′N 111°00′E	SIN	OUC[b], China
A. tibetiana	Lagkor Lake, China	32°02′N 84°9′E	TIB	OUC, China
A. sorgeloosi	Haiyan Lake, China	36°48′N 100°41′E	SOR	IATS[c], Spain
A. amati	Kazakhstan[d]	48°0′N 68°0′E[d]	AMA	IATS, Spain
A. urmiana	Urmia Lake, Iran	37°42′N 45°22′E	URM	HTOU[e], China
A. monica	Mono Lake, USA	38°01′N 119°01′W	MON	ARC, Belgium
A. franciscana	San Francisco Bay, USA	37°30′N 122°02′W	FRA	ARC, Belgium
A. persimilis	Buenos Aires, Argentina	34°36′S 58°26′W[f]	PER	ARC, Belgium
Diploid parthenogenetic lineage	Ga Hai Lake, China	37°08′N 97°33′E	DI	OUC, China
Triploid parthenogenetic lineage	Aibi Lake, China	44°53′N 83°00′E	TRI	OUC, China
Tetraploid parthenogenetic lineage	Hoh Lake, China	36°56′N 98°14′E	TETRA	OUC, China
Pentaploid parthenogenetic lineage	Yinggehai Saltern, China	18°31′N 108°44′E	PENTA	OUC, China

[a] *Artemia* Reference Center, [b]Ocean University of China, [c]Institute of Aquaculture Torre de la Sal, [d]Geographic data only refer to Kazakhstan (see Asem et al., 2023), [e]Hainan Tropical Ocean University, [f]geographic coordinates only refer to Buenos Aires, this sample has been registered under ARC1321 from an unknown locality in Buenos Aires (Mahieu, per. com. 2023)

Bioinformatics analysis

Quality control and sequence assembly

Adapter residues were removed from the sequencing data by Novogene Co., and only sequences consisting of both paired reads were used for further analyses. Quality control was performed with the software package FastQC [65], as in Asem et al. [61]. For mitogenome assembly of the Asian species and parthenogenetic lineages, the mitogenomes of both *A. sinica* (GenBank accession no. MK069595; [64]) and *A. urmiana* (GenBank accession no. MN240408; [61]) were used as reference sequences. The *A. franciscana* mitogenome (GenBank accession no. X69067; [66]) served as a reference sequence to assemble that of the *A. salina* and American species. Bowtie v2.2.9 software [67] and Geneious R9.1 software [68] were used for sequence mapping and reference-based assembly, respectively, with parameter settings as in Asem et al. [4]. To confirm mitogenome sequence validity (circular form), each mitogenome was assembled twice and considered in two different positions with a 5,000 bp difference.

Gene identification and annotation

The secondary structure and position of mitogenomic transfer RNA (tRNA) genes were determined with ARWEN online software using default parameters (http://130.235.244.92/ARWEN/). Nucleic acid folding and hybridization of the tRNA sequences were predicted using the mfold online platform (http://www.unafold.org/mfold/applications/rna-folding-form.php) [69]. Ribosomal RNA genes (rRNAs) and protein-coding genes (PCGs) were annotated, based on gene order in the reference mitogenomes, followed by NCBI's BLAST online platform (https://blast.ncbi.nlm.nih.gov), using default parameters. The BioEdit v.7.2 software [70] was used to help determine the orientation and position of rRNAs and PCGs, based on multiple sequence alignments between the reference mitogenomes and all examined sequences in this study. Finally, the ExPASy online program (https://web.expasy.org/translate/) was utilized (setting: "invertebrate mitochondrial" codes) to translate PCG sequences into amino acid sequences, to ensure each PCG can encode a functional protein.

The nucleotide composition (AT% and GC%) and codon usage were determined with DAMBE 7 [71]. The AT- and GC- skews were also assessed, as described in Perna and Kocher [72]. Relative synonymous codon usage (RSCU) patterns variation between *Artemia* species and parthenogenetic lineages were determined with principal component analysis (PCA) using SPSS v18 software.

MEGA X software [73] was employed to calculate the percentage of variable sites (VS), as well as the pairwise interspecific genetic distances (D) and nucleotide diversity (ND) for each rRNA, PCG, and for a concatenated sequence of two rRNAs and 13 PCGs from both *Artemia* species and parthenogenetic lineages, according to the uncorrected p-distance nucleotide model ([74], Meier, per. com). Heat map values were illustrated using the Plotly online software (https://chart-studio.plotly.com).

Phylogenetic analysis

Phylogenetic relationship analysis between *Artemia* members was performed on a concatenated dataset, including two rRNAs and 13 PCGs, using Maximum Likelihood (ML) and Bayesian Inference (BI) as implemented in RAxML-HPC BlackBox 8.2.12 and MrBayes on XSEDE 3.2.7a, respectively [75]. Both methods were conducted on the CIPRES Science Gateway online platform (https://www.phylo.org/portal2). *Streptocephalus cafer* (GenBank accession no. NC_046688; [76]) was chosen as an outgroup.

The best fitting nucleotide substitution model of DNA was calculated following MrModeltest 2.2 software [77]) The GTR + I + G was chosen as the best fit model for both methods (ML: bootstrap replicates: 1,000; BI: nst = 6, rates = invgamma; mcmcp ngen = 10,000,000 samplefreq = 100 nchains = 4, sump burnin = 25,000, sumt burnin = 25,000). FigTree v1.4.4 was used to visualize the phylogenetic trees [78]. For the ML bootstraps, values < 70 were regarded as low and ≥ 95 as high [79]. For the BI posterior probabilities, the values < 0.94 were considered low and ≥ 0.95 as high [80].

The SAW method (see [81]) was used to evaluate if "long branch length" was systematic error as "long branch attraction" (LBA) ([82, 83], Bergsten, per. com).

Divergence time estimation using BEAST

Manzi et al. [84] reported fossil *A. salina* from Cyprus without any evidence to its identity; it is only a part of a putative anostracan thorax. *Artemia*, *Branchinectella media* (Schmankewitsch, 1873) and *Phallocryptus spinosa* (Milne-Edwards, 1840) are hypersaline anostracans, and all are reported from the Mediterranean Basin, where they may coexist (see [85, 86]). There is no taxonomic evidence to accept Manzi's finding is *Artemia*, let alone "*Artemia salina*". Therefore, divergence time was calibrated at 145 Mya, based on the age of a fossil of *Daphnia* Müller, 1785 (Crustacea: Anomopoda) ([87], see also [22]). Bayesian tree reconstruction and divergence times were calculated using the software BEAST v1.10.1 [88]. We tested the "relaxed clock" and "strict clock", with the following additional parameters: nucleotide substitution model = GTR with four rate categories; Gamma + Invariant Sites heterogeneity among species; Tree Prior = Yule process ([89, 90], see also [91]); Random starting tree; Ancestral State Reconstruction = Reconstruct states at ancestor and Tree Root [92]. XML files for all BEAST runs were created using BEAUti v1.10.1 [88].

Posterior probability distributions of parameters were calculated by Markov Chain Monte Carlo (MCMC) sampling [88]. All runs were combined after a 10% burn in using LogCombiner v1.10.1 [88]. TRACER v.1.7.2 [93] was used to verify the stationary distribution of acceptable MCMC steps mixing, and to ensure appropriate sampling of each parameter (i.e., effective sampling size (ESS) > 200) (https://beast.community/ess_tutorial, see also [22, 91, 94, 95]. TreeAnnotator v1.10.1 [88] was utilized to annotate the maximum clade credibility tree (see [22]). The phylogenetic tree and clade divergence times were visualized using FigTree v 1.4.0 [78].

The analysis was run using "strict clock" over 40 million generations (the first step that ESS > 200), taking samples every 1,000 generations using BEAST (for more information see Results and Discussion).

Results

Mitogenome organization and composition

The mitogenomes of the nine species and four parthenogenetic lineages represent typical circular DNA, including 22 tRNAs, 2 rRNAs, 13 PCGs and a noncoding control region exhibiting a total length ranging from 15,433 bp (SAL1, GenBank accession no.: OR423222) to 15,829 bp (FRA1, GenBank accession no.: OR423224), respectively. The gene arrangement is identical in all *Artemia* mitogenomes, where nine PCGs and 13 tRNAs are coded on the heavy (H-) strand while the other genes (both rRNAs, four PCGs, and nine tRNAs) are encoded on the light (L-) strand (Table S1A-V). The mitogenome size and nucleotide compositions PCGs + rRNAs sequences are given in Table 2.

Six start codons, including ATG, ATC, ATT, GTG, ATA and TTG, were recognized in *Artemia* mitogenomes.

Table 2 Detailed information of the mitogenome sequences from nine species and four parthenogenetic lineages of *Artemia* in this study (see Table 1)

Taxon status	A	B	C	D	E	F	G	H	I
A. salina	SAL1	15,433	12,415	1,467	55.21	−0.1885	−0.0569	OR423222	this study
	SAL2	15,434	12,415	1,468	55.21	−0.1885	−0.0569	OR423223	this study
A. sinica	SIN1	15,689	12,420	1,682	63.86	−0.1713	−0.0470	OP800906	this study
	SIN2	15,687	12,420	1,680	63.86	−0.1713	−0.0470	OP805358	this study
A. tibetiana	TIB1	15,626	12,423	1,616	61.78	−0.1657	−0.0549	OP168928	[4]
	TIB2	15,638	12,423	1,623	61.80	−0.1661	−0.0555	OR423229	this study
A. sorgeloosi	SOR1	15,803	12,423	1,790	62.05	−0.1651	−0.0482	OP156999	[4]
	SOR2	15,754	12,423	1,741	62.03	−0.1655	−0.0482	OR423219	this study
A. amati	AMA1	15,679	12,423	1,662	61.94	−0.1669	−0.0515	OP142420	[4]
	AMA2	15,680	12,423	1,663	61.99	−0.1676	−0.0502	OR423218	this study
A. urmiana	URM1	15,699	12,426	1,683	61.92	−0.1660	−0.0530	MN240408	[4]
	URM2	15,675	12,424	1,664	61.87	−0.1695	−0.0490	OR423228	this study
A. monica	MON1	15,825	12,424	1,817	63.59	−0.1740	−0.0368	OR423226	this study
	MON2	15,824	12,424	1,816	63.60	−0.1729	−0.0390	OR423227	this study
A. franciscana	FRA1	15,829	12,424	1,820	63.81	−0.1753	−0.0342	OR423224	this study
	FRA2	15,827	12,424	1,819	63.81	−0.1753	−0.0342	OR423225	this study
A. persimilis	PER1	15,764	12,398	1,796	63.91	−0.1666	−0.0213	OR423220	this study
	PER2	15,766	12,398	1,796	63.98	−0.1678	−0.0197	OR423221	this study
Diploid parthenogenetic lineage	DI1	15,666	12,423	1,661	62.18	−0.1673	−0.0481	OR423214	this study
	DI2	15,668	12,423	1,663	62.19	−0.1673	−0.0478	OR423215	this study
Triploid parthenogenetic lineage	TRI1	15,679	12,423	1,662	62.25	−0.1665	−0.0490	OR423216	this study
	TRI2	15,680	12,423	1,663	62.25	−0.1665	−0.0490	OR423217	this study
Tetraploid parthenogenetic lineage	TETRA1	15,683	12,422	1,674	63.81	−0.1721	−0.0475	OR423213	this study
	TETRA2	15,693	12,422	1,684	63.78	−0.1715	−0.0497	OP805359	this study
Pentaploid parthenogenetic lineage	PENTA1	15,690	12,422	1,681	63.80	−0.1708	−0.0513	OP830835	this study
	PENTA2	15,693	12,422	1,684	63.80	−0.1708	−0.0513	OP830836	this study

A: Abbreviation for examined sequences (abbreviations listed in Table 1), B: Total mitogenome length (bp), C: PCGs + rRNAs length (bp), D: control region length (bp), E: A + T%, F: AT–skew, G: GC–skew, H: GenBank accession no., I: References (The values of D, E and F refer to concatenated sequences of PCGs and rRNAs)

ATG codon was identified as common and rare start codons with a frequency of 48.52%. The protein-coding genes *COX1*, *COX3*, *CYTB* and *ND1* were initiated by a common ATG codon in all species and parthenogenetic lineages. The rare TTG start codon was only identified in the *ND5* and *ND6* protein coding gene (Fig. 1, Tables S2, S3, S4). Two stop codons, TAA and TAG, and an incomplete T stop codon were identified with frequencies of 51.48%, 17.16%, and 31.36%, respectively. The TAA stop codon was identified in all *ATP6* protein-coding genes and the incomplete T stop codon was observed in genes *COX1*, *COX2*, *ND5* and *ND4* of all *Artemia* mitogenomes (Fig. 1, Tables S2, S3, S4).

Artemia mitogenomic tRNAs have the typical cloverleaf secondary structure, except tRNA-$Ser_{1,}$ which lacks a D-arm structure (Fig. 2). The most and least conserved tRNA sequences belong to tRNA-Met (57 conserved sites *vs.* 65 total sites, 87.69%) and tRNA-Glu (38 conserved sites *vs.* 66 total sites, 57.58%), respectively. An abnormal structure was detected in the acceptor stem of tRNA-Ser_1 in some taxa (*A. tibetiana*, *A. urmiana*, *A. amati*, *A. sorgeloosi*, di- and triploid parthenogenetic lineages) due to a lack of linking between second pair nucleotides (G and A) using the ARWEN online software (Fig. 3A). The possibility of a secondary structure of tRNA-Ser_1 was reconsidered by using the mfold online platform, which demonstrated that the ARWEN predicted secondary structure could not be a valid folding. The acceptor stem secondary structure was rearranged and confirmed via the mfold online platform as shown in Fig. 3B. A similar condition was recognized in the tRNA-Leu_2 acceptor stem in the *A. persimilis* mitogenome (Fig. 4 A, B).

The nucleotide compositions of the concatenated PCGs + rRNAs sequences are depicted in Fig. 5 (Supplementary material Table S5). GC% and AT% values demonstrate that *Artemia* members cluster in three groups. Group A members are American origin *Artemia* (*A. monica*, *A. franciscana* and *A. persimilis*) and some Asian origin *Artemia (A. sinica*, tetra- and pentaploid parthenogenetic lineages) (Fig. 5B). All Group B members are *Artemia* of Asian origin (*A. urmiana*, *A. tibetiana*, *A. sorgeloosi*, *A. amati*, di- and triploid parthenogenetic lineages) (Fig. 5C). The Mediterranean *A. salina* is in a distinct group alone (Group C) (Fig. 5A). The GC- and AT-skew values are negative in all PCGs + rRNAs sequences (Supplementary material Table S6). Although *Artemia* species and parthenogenetic members have a wide distribution based on GC- and AT-skews, *A. persimilis* and *A. salina* are notably more isolated than others (Fig. 5D).

Thirteen shared protein-coding genes from each individual (totaling 26 individuals, including two specimens each of 13 species and parthenogenetic lineages) were used to analyze the codon usage of *Artemia* mitogenomes. UUU (Phe, F) and AUU (Ile, I) were the most representative codons, with a total of 5,462 (ranging from 173 to 228) and 5,328 records (ranging from 135 to 223), respectively. AGG (Ser, S) was the least common with 158 records (ranging from 1 to 8). These most representative and least commonly used codons were noted in *A. persimilis*: UCU (Ser, S) with a usage count of 141 in both PER1 (RSCU: 3.00) and PER2 (RSCU:2.99) and AGG (Ser, S) with a usage count of 1 in PER1 (RSCU: 0.021) and 2 in PER2 (RSCU: 0.042) (Fig. 6). Supplementary material Tables S7–S9 provides details of RSCU listed for each individual of each species and parthenogenetic lineage. The PCA of RSCU is shown in Fig. 7. The first and second components represent 50.61% and 20.87% of the variation, respectively, with AUC (0.935), AUU (−0.935) and GUA (−0.920) contributing to the first component and CAC (0.919), CAU (−0.919) and GCG (−0.825) contributing to the second component. PCA showed four groups, with those *Artemia* of Asian origin clustered in two relatively homogenous groups (Groups B and D). American origin species clustered together (Group A), while the Mediterranean *A. salina* was significantly isolated as a distinct group (Group C).

Intraspecific diversity and genetic distance

The percentage of variable sites (VS) and the nucleotide diversity (ND) results are summarized for each PCG, rRNA gene, and concatenated sequences of PCGs and rRNAs in Fig. 8. There is likely a positive correlation between the two parameters, as they seem to move together. The highest and lowest values of VS and ND belong to *ATP8* / *ND6* and *COX1* / *COX2* protein-coding genes, respectively (Fig. 8 and Table S10). The pairwise interspecific genetic distances based on 13 PCGs, two rRNAs and *Artemia* mitogenomes (PCG + rRNA genes) are shown in Fig. 9 (see also Table S11). The greatest distances were found in *A. persimilis* and *A. salina* for most genes, except for *ATP8*, *ND4L* and *ND6* PCGs and *12S* rRNA genes, where the highest values referred to the genetic distance between *A. persimilis* and *A. franciscana*/*A. monica*, di-/triploid parthenogenetic lineages, *A. sorgeloosi* and the pentaploid parthenogenetic lineage, respectively. The lowest values were shared between diploid and triploid lineages (*ND2*, *COX2*, *ATP8*, *COX3*, *ND3*, *ND5*, *ND4L*, *ND6*, *16S*, *12S*, PCG + rRNA genes), and between tetraploid and pentaploid lineages (*COX1*, *ATP6*, *ND4*, *CYTB*, *ND1*).

Phylogeny and origin

Figure 10A represents the phylogenetic relationships among all species and four parthenogenetic lineages using mitogenome sequences. Both reconstructed trees

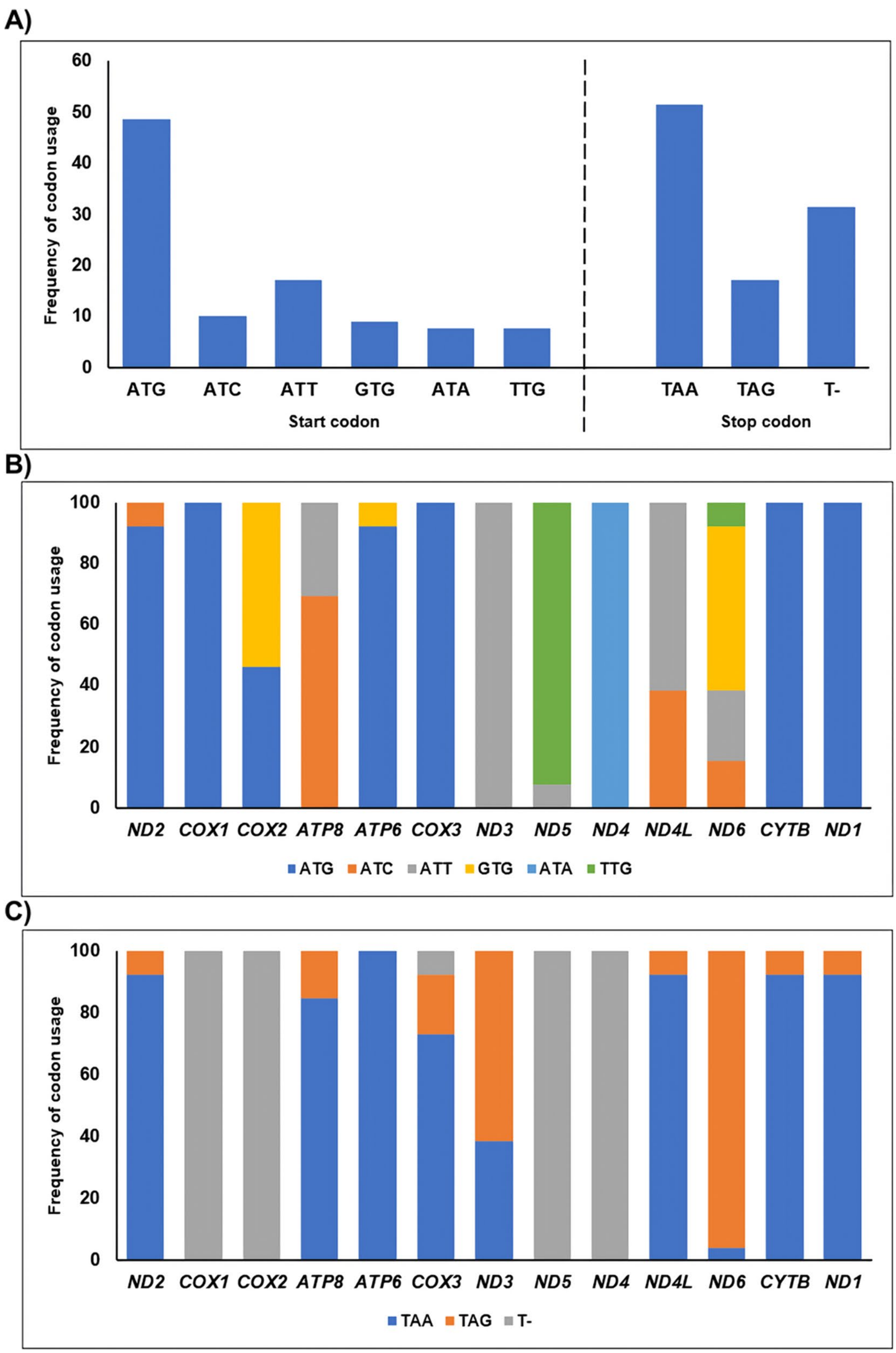

Fig. 1 Distribution of start and stop codon usages in the *Artemia* mitogenome. **A** frequency of start and stop codon usages; **B**) frequency of start codon usages in each PCG; **C**) frequency of stop codon usages in each PCG

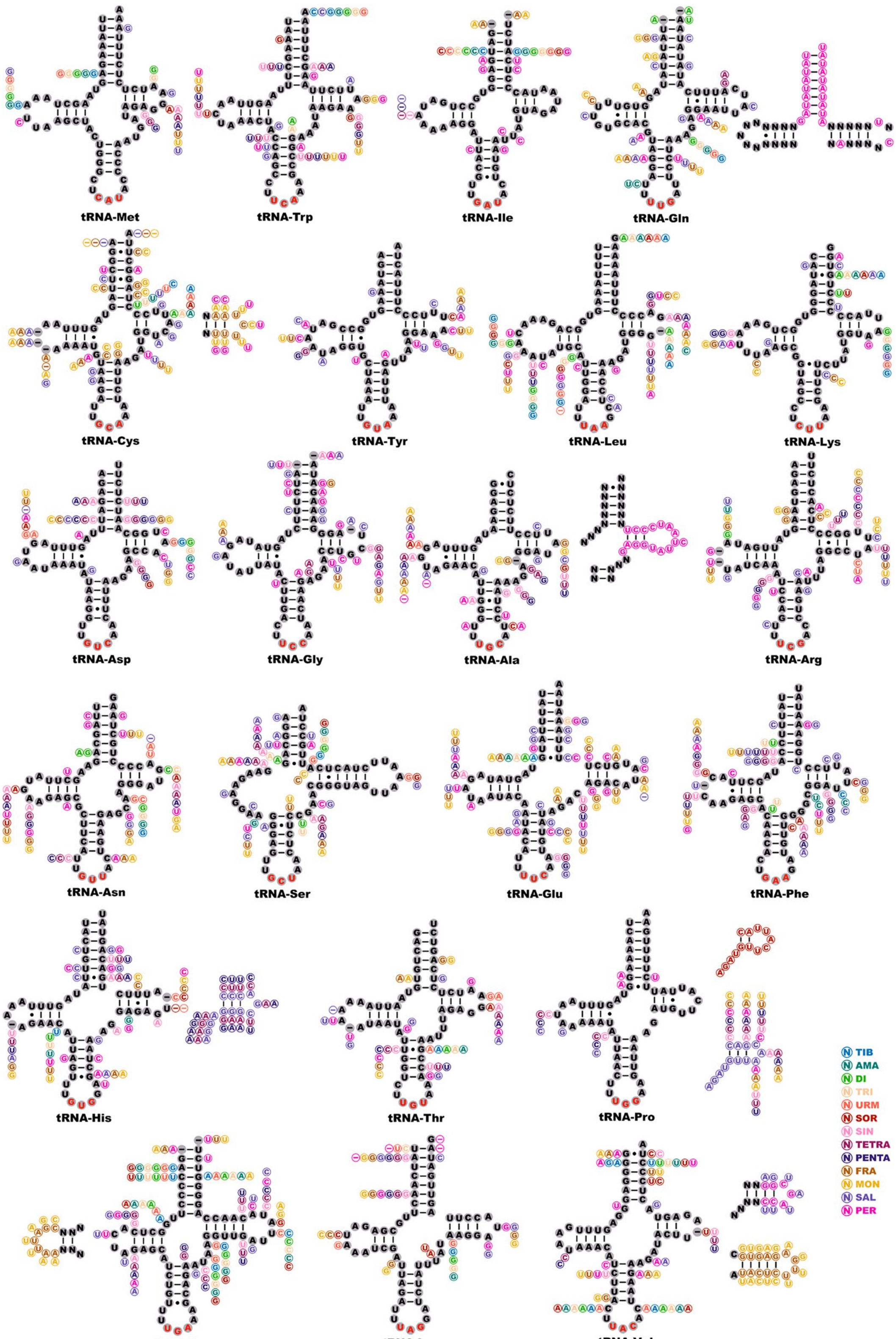

Fig. 2 The predicted secondary structure of tRNA genes in the *Artemia* mitogenomes of the 13 investigated taxa. Any alteration, deletion and insertion has been labeled (abbreviations listed in Table 1)

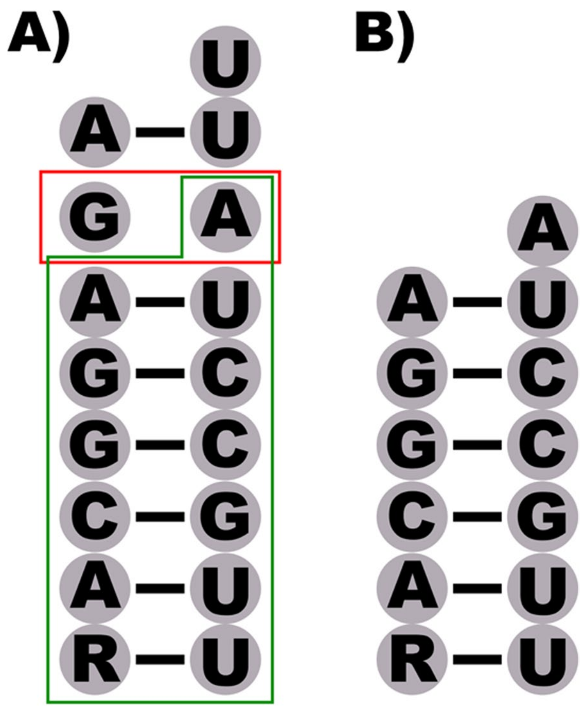

Fig. 3 The predicted secondary structure of the acceptor stem of tRNA-Ser_1 (*A. tibetiana*, *A. urmiana*, *A. amati*, *A. sorgeloosi*, di- and triploid parthenogenetic lineages). A) output of the ARWEN software; B) the revised structure (the red rectangle and green polygon show unlinked nucleotides and the position of the revised acceptor stem in the secondary structure, respectively)

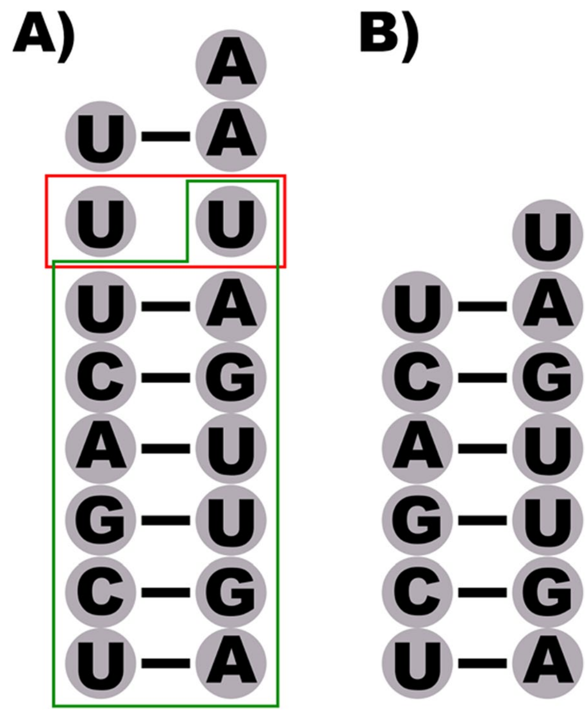

Fig. 4 The predicted secondary structure of the acceptor stem of tRNA-Leu_2 of *A. persimilis*. **A** output of the ARWEN software, **B**) the revised structure (the red rectangle and green polygon show unlinked nucleotides and the position of the revised acceptor stem in the secondary structure, respectively)

(ML and BI) show the same topology, with *A. persimilis* located as a basal clade. The phylogenetic trees contain a "long branch length" with *A. salina* (Fig. 10A). Following the SAW method (see Materials and Methods) the observed "long branch length" should be considered as a true organismal phylogeny, not a long branch attraction (LBA) as a form of systematic error (Figs. 10B-E), with *A. salina* sister to the North American *Artemia*, which includes separate, distinct, and well-supported clades for *A. monica* and *A. franciscana*. Asian *Artemia* is divided in two major clades. The first clade contains *A. sinica*, plus tetra- and pentaploid parthenogenetic lineages. The second clade consists of *A. sorgeloosi*, *A. urmiana*, *A. amati*, *A. tibetiana*, and di- and triploid parthenogenetic lineages. *Artemia sinica* and *A. sorgeloosi* are sisters to the Asian clades, respectively. It seems that the observed difference in the topology of the mitochondrial phylogeny trees is due to the neglect of the "long branch length" in previous studies (see introduction).

Divergence time

Ten setting analyses (10 to 100 million generations, taking samples every 1,000 generations) were performed following the "relaxed clock" method. In all ten analyses, the ESS for several parameters was lower than 200 (most of them were also lower than 100; see Materials and Methods). The topology of estimated trees using "relaxed clock" method were unreliable and displayed a false inference, so that *A. sorgeloosi* was located as a basal clade for American *Artemia*. Additionally, *A. sinica* and tetra-/pentaploid parthenogenetic lineages were located between them (e.g., see Fig. S1). This is in contrast with the results of phylogeny and genetic distance between *Artemia* members in the present study and former studies. Therefore the "strict clock" method was chosen to estimate divergence time (for more information see Discussion).

Following the result of "strict clock" method, the diversification of *Artemia* began *ca.* 33.97 Mya (30.74–37.27 Mya; node B) in the Paleogene Period (Early Oligocene–Late Eocene) following the divergence of the ancestral lineage of *A. persimilis* from the other taxa (Fig. 11). The second division occurred between ancestral lineages of Mediterranean *A. salina* and the other taxa *ca.* 26.32 Mya (23.57–28.96 Mya; node C) during the Paleogene Period (Early Miocene–Early Oligocene). The divergence between North American and Asian taxa took place in the Early Miocene, *ca.* 21.10 Mya (18.86–23.32

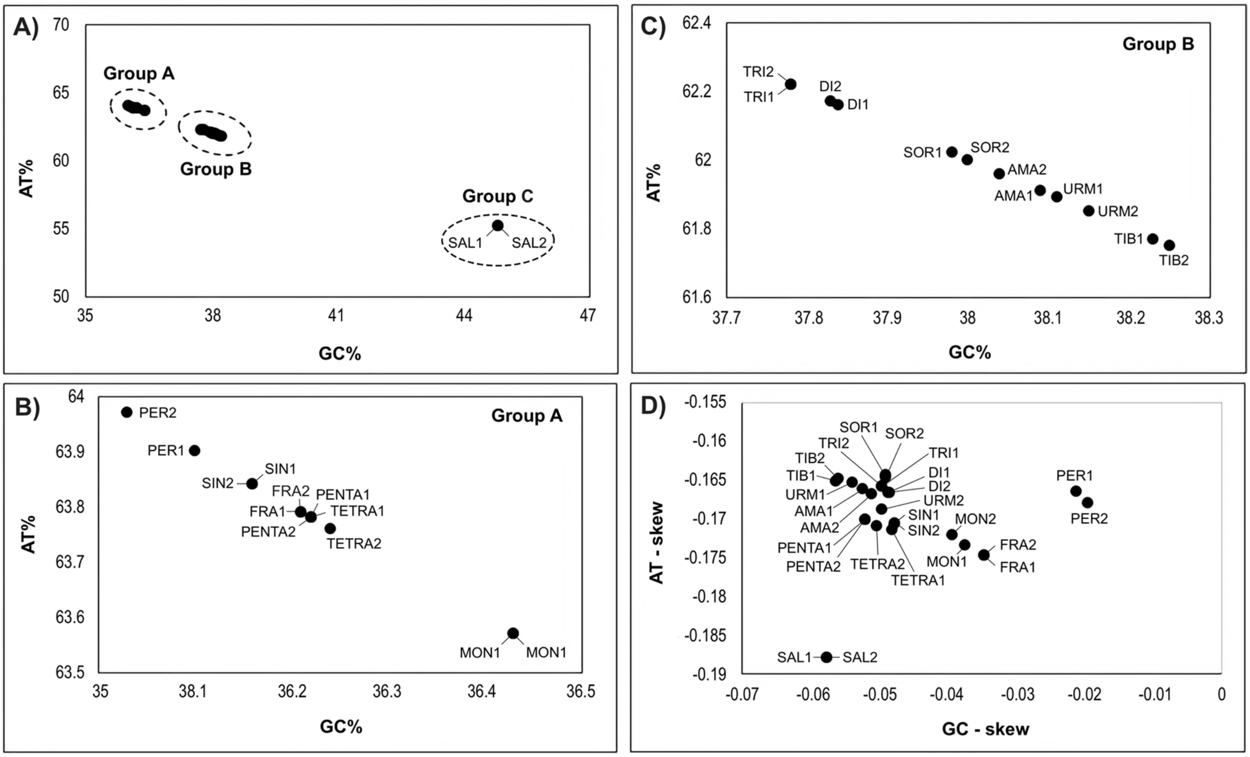

Fig. 5 Distribution of *Artemia* taxa on scatter plots based on **A**; **B**; **C**) GC%- and AT% and **D**) GC- and AT-skew values of PCGs + rRNAs (abbreviations listed in Table 2)

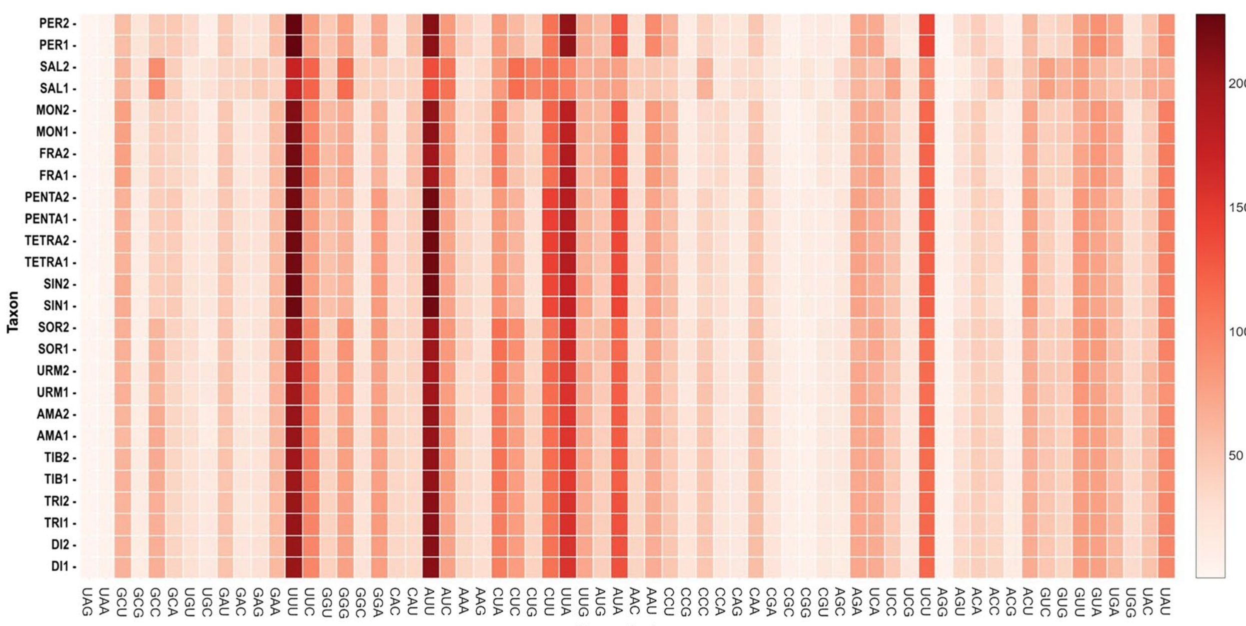

Fig. 6 Heat-map values for "number of usages per codon", based on 13 PCGs of the *Artemia* mitogenomes

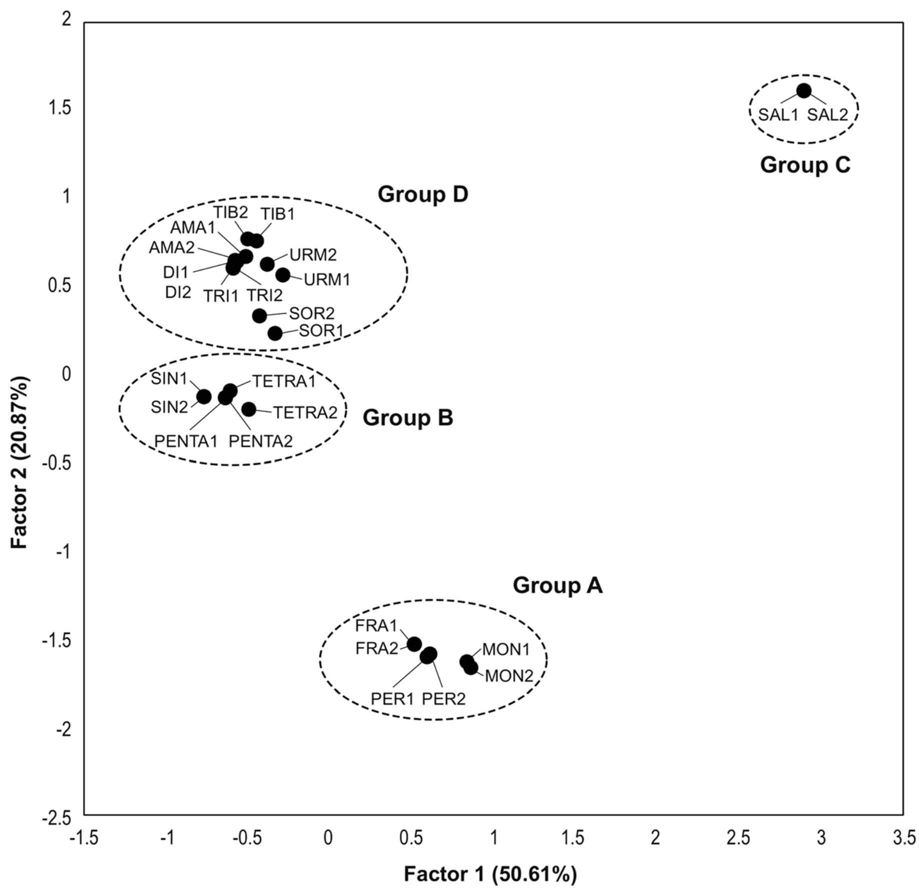

Fig. 7 PCA plot based on RSCU value for 13 PCG of the *Artemia* mitogenomes (abbreviations listed in Table 2)

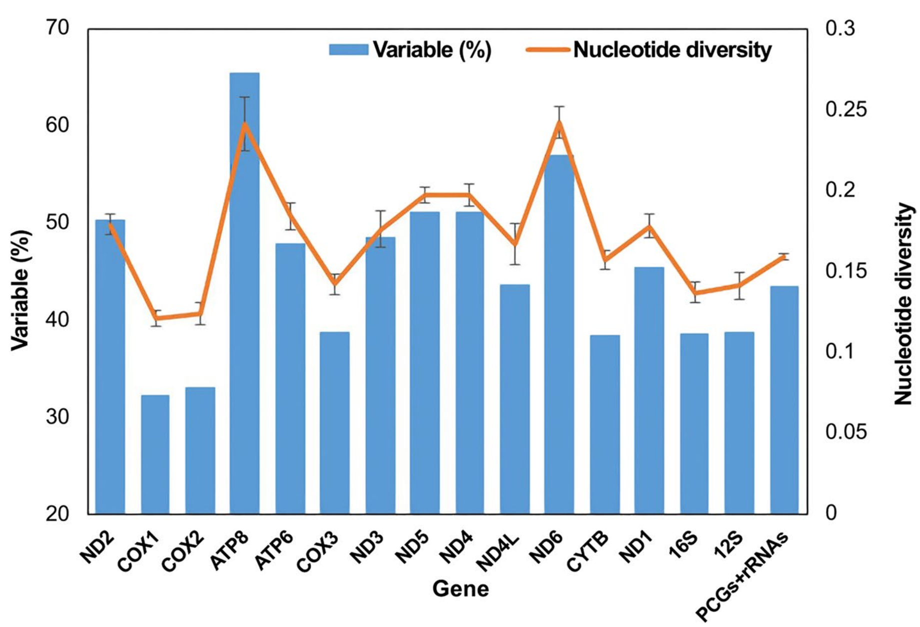

Fig. 8 Percentage of variable sites and nucleotide diversity for each PCG, rRNA and PCGs + rRNAs genes

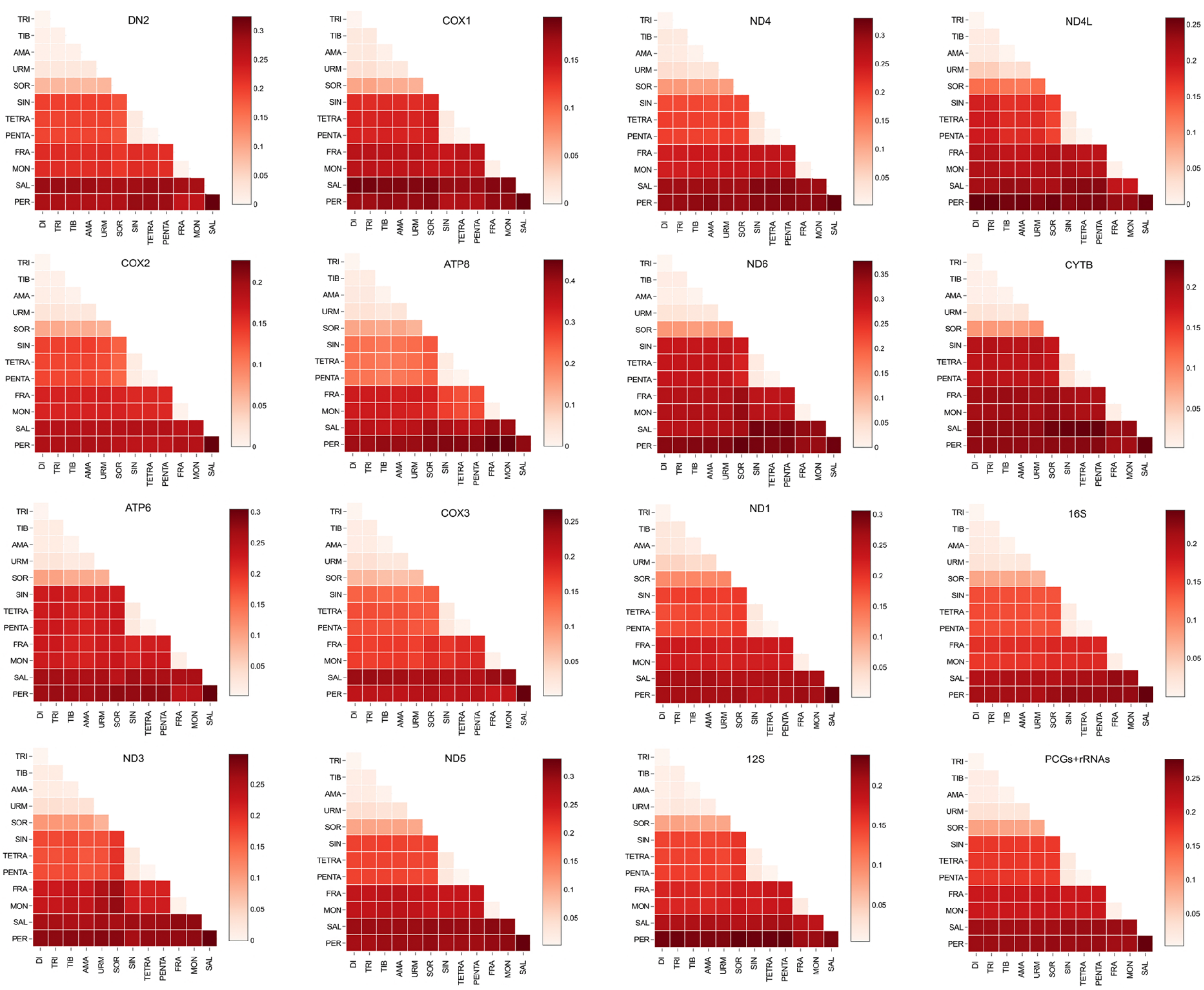

Fig. 9 Heat-map values of interspecific genetic distances based on 13 PCGs and two rRNAs separately and concatenated sequence of PCG + rRNA genes (X and Y axes are referred to *Artemia* taxa, abbreviations listed in Table 1)

Mya; node D). Based on our calibration, diversification in common ancestors of North American (*A. monica* and *A. franciscana*) and Asian *Artemia* appears to have occurred *ca.*0.44 Mya (0.39–0.54 Mya) in the Late Pleistocene (node E) and *ca.* 14.27 Mya (12.73–15.96 Mya; node F) in the Middle Miocene, respectively. The second Asian clade formed *ca.* 4.85 Mya (4.23–5.49 Mya; node H), mainly in the Early Pliocene. Although Pleistocene diversification of the tetraploid parthenogenetic lineage was earlier than the pentaploid parthenogenetic lineage (Holocene) (0.01–0.15 Mya *vs.* 0.00–0.008 Mya), diversification of diploid and triploid parthenogenetic lineages occurred in the Holocene at the same time (0.0001–0.01 Mya, 0.0008–0.01 Mya, respectively). The data indicates that initial diversification to *A. sinica, A. franciscana, A. salina,* and di-/tri-/pentaploid parthenogens occurred during the Holocene, while divergence of other taxa (consisting of *A. urmiana, A. tibetiana, A. Amati, A. sorgeloosi, A. persimilis, A. monica* and tetraploid parthenogens) occurred during the Late Pleistocene.

Discussion

Mitogenome organization and composition

We sequenced and assembled the mitogenomes of all described *Artemia* species and parthenogenetic lineages (with their ploidies identified), assuming that the complete mitogenome will provide better phylogenetic resolution and divergence time relative to traditional single mitochondrial or nuclear markers previously considered [51, 52].

The *Artemia* mitochondrial gene order is uniform with the ancestral Pancrustacea model, including 22 tRNAs, 2 rRNAs and 13 PCGs [96]. However, a slight variation was observed in mitogenome length (15,433 *vs.* 15,829 bp), though concatenated sequences of PCGs and rRNAs exhibit a conserved size (12,398 *vs.* 12,426 bp).

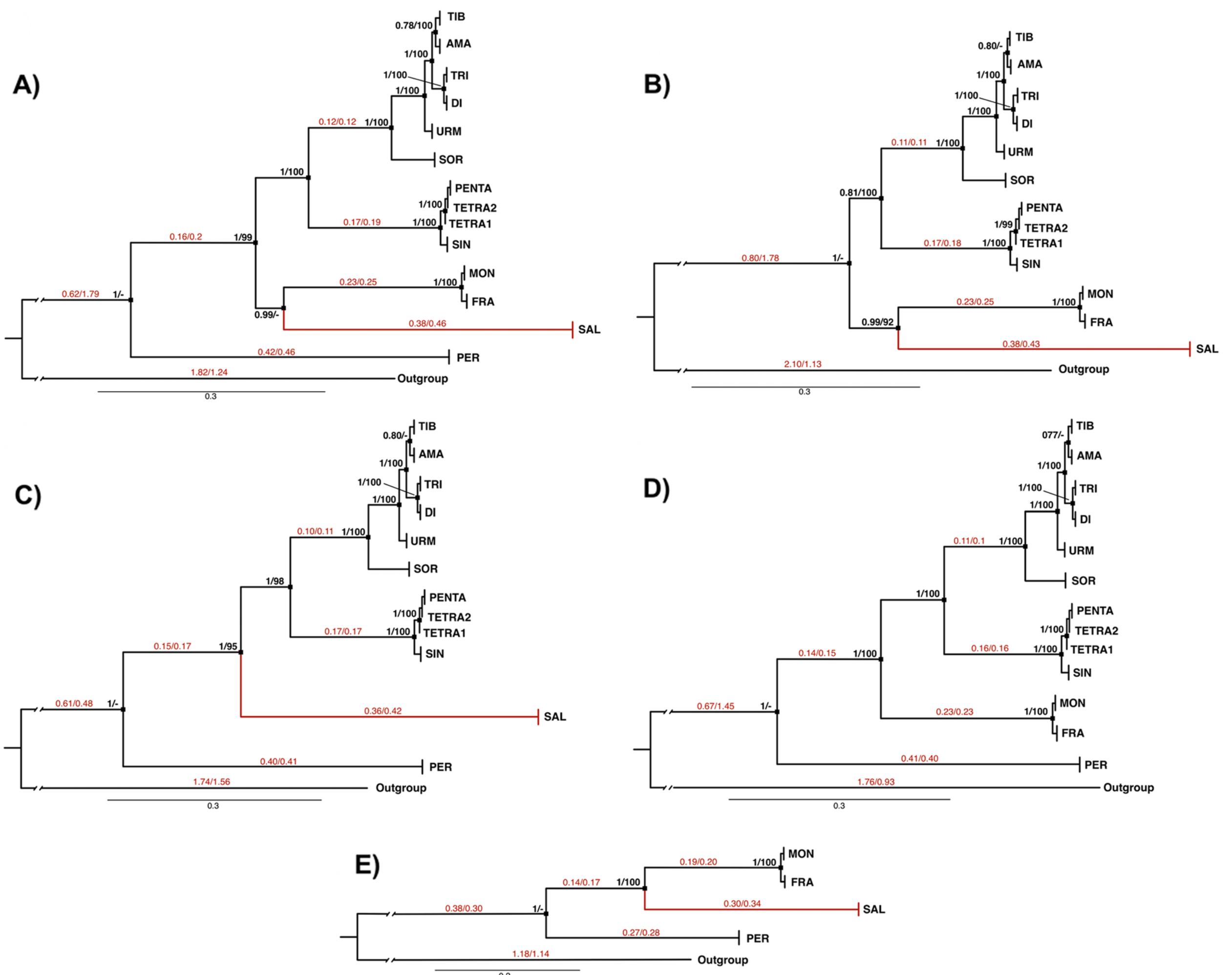

Fig. 10 Mitogenomic phylogeny of *Artemia* based on Bayesian inference (BI) and Maximum-Likelihood (ML). A) using all *Artemia* taxa B) following the SAW method, the *A. persimilis* clade is not considered C) following the SAW method, the North American clade not considered D) long branch length (*A. salina* clade) not considered (Bergsten, personal communication, 2023) E) Asian clade not considered (Bergsten, personal communication, 2023). Numbers above the branches in red show the length of major branches (left: BI and right: ML). The number behind major nodes denotes posterior probabilities. The Bayesian support (left) and ML bootstrap values (right) are shown for each major node. long branch length is indicated by a red branch (abbreviations listed in Table 1)

Previous studies showed that the control region, regulating mtDNA replication and transcription [97], is less conserved in Asian *Artemia* [4, 61]. Our results show that sequences of this region differ by 19.4% among *Artemia* species (1,467 *vs.* 1,820 bp). Thus, we conclude that the *Artemia* control region is not conserved. This mitochondrial variability in the cell "energy factory" may potentially influence the expression of key genes [4, 61, 98], and the metabolic paths generating energy for *Artemia* adaptation to the harsh hypersaline conditions [4]. The role of mitochondrial genes in the *Artemia* adaptation to the harsh conditions of hypersaline environments needs further experimental assessment.

The mitogenome nucleotide composition differs across taxa [72, 99–102], likely due to differential selective pressures of individuals adapted to ecologically heterogeneous and stringent environments, with habitat-specific mutation rates and DNA repair mechanisms (see [23, 101, 102]). The ecological barrier between *A. monica* and *A. franciscana* justifies their reproductive isolation, criteria used for considering them as independent species following the "Biological Species" concept. Our findings reveal clear mitogenome composition differentiation (AT-/GC- content, RSCU and structure of tRNA-Gly, tRNA-Arg and tRNA-Asn) of *A. monica* and *A. franciscana*.

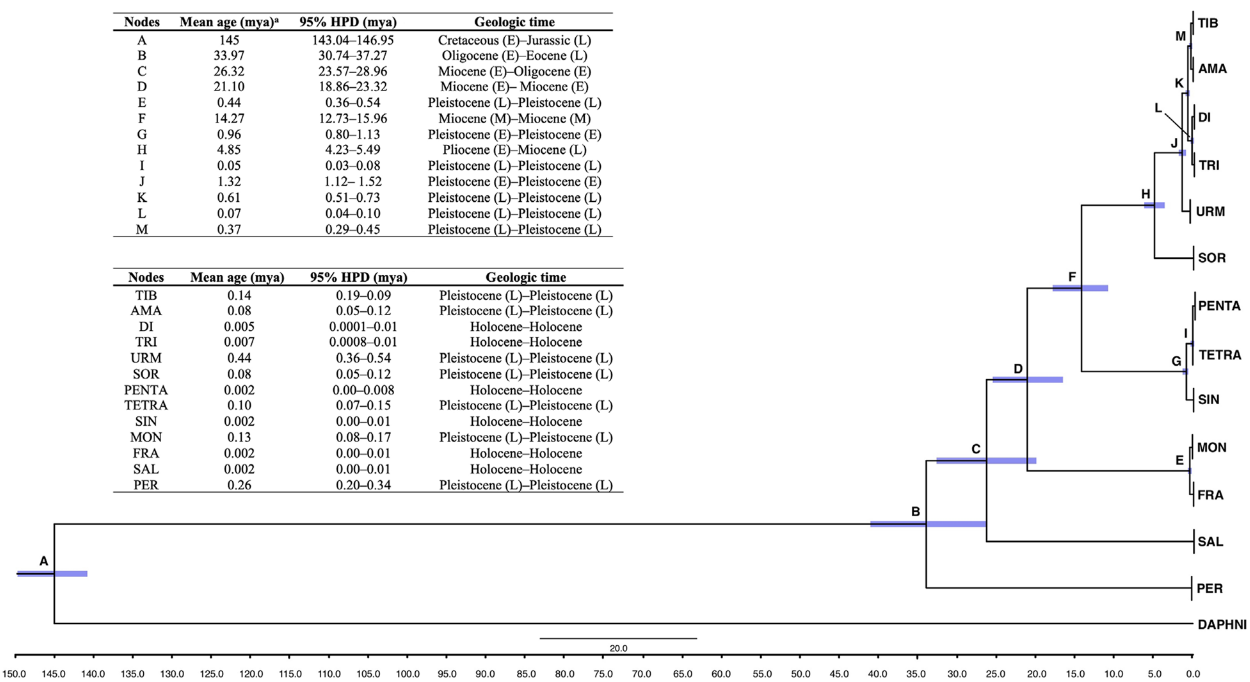

Nodes	Mean age (mya)[a]	95% HPD (mya)	Geologic time
A	145	143.04–146.95	Cretaceous (E)–Jurassic (L)
B	33.97	30.74–37.27	Oligocene (E)–Eocene (L)
C	26.32	23.57–28.96	Miocene (E)–Oligocene (E)
D	21.10	18.86–23.32	Miocene (E)– Miocene (E)
E	0.44	0.36–0.54	Pleistocene (L)–Pleistocene (L)
F	14.27	12.73–15.96	Miocene (M)–Miocene (M)
G	0.96	0.80–1.13	Pleistocene (E)–Pleistocene (E)
H	4.85	4.23–5.49	Pliocene (E)–Miocene (L)
I	0.05	0.03–0.08	Pleistocene (L)–Pleistocene (L)
J	1.32	1.12– 1.52	Pleistocene (E)–Pleistocene (E)
K	0.61	0.51–0.73	Pleistocene (L)–Pleistocene (L)
L	0.07	0.04–0.10	Pleistocene (L)–Pleistocene (L)
M	0.37	0.29–0.45	Pleistocene (L)–Pleistocene (L)

Nodes	Mean age (mya)	95% HPD (mya)	Geologic time
TIB	0.14	0.19–0.09	Pleistocene (L)–Pleistocene (L)
AMA	0.08	0.05–0.12	Pleistocene (L)–Pleistocene (L)
DI	0.005	0.0001–0.01	Holocene–Holocene
TRI	0.007	0.0008–0.01	Holocene–Holocene
URM	0.44	0.36–0.54	Pleistocene (L)–Pleistocene (L)
SOR	0.08	0.05–0.12	Pleistocene (L)–Pleistocene (L)
PENTA	0.002	0.00–0.008	Holocene–Holocene
TETRA	0.10	0.07–0.15	Pleistocene (L)–Pleistocene (L)
SIN	0.002	0.00–0.01	Holocene–Holocene
MON	0.13	0.08–0.17	Pleistocene (L)–Pleistocene (L)
FRA	0.002	0.00–0.01	Holocene–Holocene
SAL	0.002	0.00–0.01	Holocene–Holocene
PER	0.26	0.20–0.34	Pleistocene (L)–Pleistocene (L)

Fig. 11 A chronogram for the genus *Artemia* using the mitogenome. The blue node bars indicate 95% posterior probability intervals. (Mya: million years ago; HPD: highest posterior density, [a] nsotes to lower and upper 95% HPD intervals, abbreviations listed in Table 1). Geologic time scale was determined following the U.S. Geological Survey (https://www.usgs.gov/)

Intraspecific diversity and genetic distance

Asem et al. [61] demonstrated that the *ATP8* protein-coding gene, involved in ATP generation in the respiratory chain, exhibits a significant difference in nucleotide composition compared to other genes and ribosomal rRNA genes, and showed that the *ATP8* gene has the highest percentage of variable sites and nucleotide diversity among PCGs and rRNAs genes among *Artemia* members. The *ATP8* gene exhibits the highest genetic distance between *A. salina* and *A. monica*/*A. franciscana* (D = 0.451). In contrast, the *COX1* protein-coding gene, also playing a role in the respiratory chain, specifically in complexes III and IV, exhibits the lowest intraspecific diversity and genetic distance among *Artemia* members and bears a similar structure between tetra- and pentaploid parthenogenetic lineages (D = 0). Therefore, *ATP8* and *COX1* genes are identified as non-conserved and conserved *Artemia* mitochondrial genes, respectively, recognizing, however, that they are part of a more complex structure, function and interaction network, including nuclear control [60]. This mitogenomic comparison among *Artemia* taxa provides a more realistic approach to the mitochondrial complexity and functionality than those based on single mitochondrial genes.

Phylogeny, origin and divergence time

The "relaxed clock" method allows each lineage and branch of a phylogenetic tree to have its own evolutionary rate [103, 104] and is used when the rate variations among lineages/clades are high [104]. However, "strict clock" is suitable for low-rate variation with shallow phylogeny [105].

According to the results of the "relaxed clock" method, the phylogenetic trees are unreliable, whereas *A. sorgeloosi* was located as a basal clade for American *Artemia*. Furthermore, *A. sinica* and tetra-/pentaploid parthenogenetic lineages were located. This problem is also observed in using "relaxed clock" to estimate divergence time in the previous study, where *A. franciscana* is located as a basal clade and *A. salina* is placed between Asian *Artemia* and *A. franciscana* (see [22]). Due to low-rate variation among North American and Asian *Artemia*, and the results of the estimated tree using a "relaxed clock" model, the "strict clock" was utilized as correct model for our data set [Brown per. com.; Yang per. com.].

Because *Artemia* species and lineages are regionally distributed and adapted to harsh and ecologically variable conditions, coupled with an island biogeography-type distribution of intraspecific diversity [3–5, 27], they represent unique conditions for studying evolutionary divergence. Such evolutionary change is likely to be accelerated or affected by climate change and anthropogenic impacts [106, 107]. Consequently, some species' taxonomic status, particularly those in places difficult to access (Tibet, Kazakhstan, etc.) or less studied, is subject to debate [4, 5]. One problem is the uncoupling of evolutionary change at morphological and molecular levels, reflected by the occurrence of "sibling species", e.g., morphologically similar but genetically divergent forms, which requires calibrating gene-level molecular markers (mitochondrial and nuclear) with different mutation rates (conserved, less conserved). In the late 1980s, *Artemia* had been confusingly referred to as a genus containing "sibling species" [108–110]. However, they are distinguishable morphologically using laboratory-cultured individuals [see 4]. Further confusion arose because most species were described typologically in the nineteenth and twentieth centuries, which led to the idea that *Artemia* was monotypic, consisting only of "*A. salina*" (see [111, 112]). This was exacerbated by toxicologists using "*A. salina*" as a test organism, without any information on the origins of their test subjects (see [2, 113]). More recently, the biological species concept (BSC) ([114], see also [115]) was applied to bisexual species of *Artemia* taxa reproductively isolated in nature [see 4]. However, the BSC has obvious limitations in *Artemia*, a genus with obligate parthenogenetic lineages [116]. Thus, our results provide a comprehensive mitogenomic phylogenetic comparison and divergence of *Artemia*, clustering the members into well-supported clades.

Artemia urmiana possesses significantly high mitochondrial and nuclear intraspecific genetic variation [4, 34]. Our results suggest that *A. urmiana* is the earliest established *Artemia* species and its intraspecific divergence dates back to *ca.* 0.44 Mya (0.36–0.54 Mya) in the Late Pleistocene. This explains the high genetic variation and population expansion of *A. urmiana*.

Sainz-Escudero et al. [117] argued "based on the occurrence of nuclear gene flow between the type locality of *A. tibetiana* and populations of *A. urmiana*" regarding the results of Maccari et al. [19], that *A. tibetiana* should be considered as a junior synonym of *A. urmiana*. Maccari et al. [19] analyzed two nuclear markers, *ITS1* and a fragment of exon-7 of $Na^{+}/K^{+}ATPase$, but Sainz-Escudero et al. did not state which nuclear markers were affected by gene flow. Asem et al. [38] demonstrated that the fragment of exon-7 of $Na^{+}/K^{+}ATPase$ is a highly conserved marker in Asian *Artemia* and cannot be considered a phylogenetic marker. Contrary to Sainz-Escudero et al.'s [117] claim, there are no shared haplotypes between *ITS1* markers of topotype *A. tibetiana* (GenBank accession no. KF736290,91; [19]) and populations of *A. urmiana* (KF736249,52; [19]). Asem et al. [4] demonstrated that *ITS1* is not an informative marker for Asian *Artemia* phylogeny. Additionally, nuclear gene pool isolation between *A. tibetiana* and *A. urmiana* has been previously documented by Nougué et al. [48] using nine SSR markers [see also 4,49]. Furthermore, morphological differentiation of *A. urmiana* in field and laboratory collections with a cercopod rudimentary/oligosetal pattern is morphological evidence to distinguish *A. urmiana* from other Asian species and parthenogenetic lineages (4, see also [116]). Although several experimental cross-studies showed weak or lack of mating isolating among Asian species, Asem et al. [4] argued that laboratory crossbreeding tests cannot prove fertility and/or infertility potential in nature. Following Sainz-Escudero et al. [117], Li et al. [118] treated *A. urmiana* and certain Tibetan populations (*A. tibetiana* and *A. sorgeloosi*) as the "*Artemia urmiana* species complex", yet at the same time demonstrated that *A. urmiana* is completely isolated from Tibetan populations based on nuclear SSR markers. The species complex designation was explained as "a neutral term for a number of related taxonomic units, most commonly involving units in which the taxonomy is difficult or confusing" following Mayr and Ashlock [119]. A species complex is not a taxonomic rank or unit of organism classification recognized by the International Commission on Zoological Nomenclature (ICZN) (see [119]). Our mitogenome phylogenetic analysis demonstrates that *A. urmiana* and *A. tibetiana* each diverged from different ancestors in different geologic periods (*ca.* 1.32 Mya in the Early Pleistocene and *ca.* 0.37 Mya in the Late Pleistocene, respectively), by which they are linked via three non-common ancestors. On the other hand, *A. urmiana*/*A. sorgeloosi* and *A. tibetiana*/*A. sorgeloosi* are connected via two and four noncommon ancestors, respectively. In conclusion, due to isolated SSR nuclear gene pools [4, 48, 49] and maternal gene pools [4, 5, 17–19, 21], and lack of common maternal ancestor, synonymisation of *A. tibetiana* or *A. sorgeloosi* with *A. urmiana* is not supported. Neither do they represent a "species complex".

A recent Asian *Artemia* phylogenetic study inferred a lack of gene flow and probable reproductive isolation in nature due to the existence of private maternal haplotypes [4, 5]. Despite this, *A. urmiana*, *A. tibetiana*, and *A. amati* exhibited low genetic distances based on partial mitochondrial markers (*COI*, *16S* and *12S*) in comparison with other anostracan families (e.g. [120]). The low genetic distances within *Artemia* are likely related to its relatively recent divergence times compared to other anostracan genera (see [22, 121–123], also reviewed in 3,4). Our dating results show that the Asian *Artemia* ancestor diverged more recently (12.73–15.96 Mya, node F) than American and Mediterranean ancestors (30.74–37.27 Mya, node B; 23.57–28.96 Mya, node C;

18.86–23.32 Mya, node D). Reanalysis of intraspecific diversity using the mitogenome data refined the genetic differentiation resolution among *A. urmiana*, *A. tibetiana* and *A. amati* (*A. urmiana*/*A. tibetiana*: D = 0.026; *A. urmiana*/*A. amati*: D = 0.027; *A. tibetiana*/*A. amati*: D = 0.007). The low genetic distance between *A. tibetiana* and *A. amati* can also be attributed to the recent divergence of *ca.* 0.37 Mya (0.29–0.45 Mya, node M) in the Late Pleistocene (see below). The significant differentiation between *A. tibetiana* and *A. amati* nuclear genomes based on SSR markers is remarkable [4, 48, 49]. Maccari et al. [19], Sainz-Escudero et al. [117] and Li et al. [118] argued the taxonomic status of Asian *Artemia* using only close genetic distances, but ignored isolation based on morphological differentiation and molecular (mitochondrial and nuclear SSR) markers. Although "genetic distance" is an important molecular tool in intra- and interspecific studies, it alone cannot be used as evidence to determine taxonomic status within *Artemia*.

Asem et al. [4] demonstrated that *A. tibetiana* and *A. sorgeloosi* are monophyletic based on nuclear genome (SSR markers) but maternally polyphyletic. They also concluded that the maternal divergence time of the *A. tibetiana* clade was after *A. sorgeloosi*, suggesting that *A. tibetiana* may have originated from a past ancestral hybridization of a maternal ancestor of *A. tibetiana* with *A. sorgeloosi* or its ancestor [4]. Our phylogenetic results confirm that each taxon arose from a distinct maternal ancestor. We also show that the maternal divergence time of the *A. tibetiana* lineage originated in the Late Pleistocene (*ca.* 0.37 Mya, node M) after the *A. sorgeloosi* lineage in the Early Pliocene/Late Miocene (*ca.* 4.85 Mya, node H), while within *A. sorgeloosi,* diversification occurred later (*ca.* 0.08 Mya) than in *A. tibetiana* (*ca.* 0.14 Mya). Thus, *A. sorgeloosi* could not have a direct evolutionary function in the origination of *A. tibetiana*. Therefore, we have revised our previous hypothesis [see 4]: we think that *A. tibetiana* may have evolved from a past ancestral hybridization via a maternal ancestor of *A. tibetiana* with a paternal ancestor of *A. sorgeloosi* on the Tibet Plateau.

As previously mentioned, *Artemia monica* and *A. franciscana* are two independent species, ecologically and reproductively isolated (see [23]), which is confirmed by the mitogenomic phylogeny showing two well-supported clades (BI/ML = 1/100) and separated from a common ancestor *ca.* 0.44 Mya (0.36–0.54 Mya, node E) in the Late Pleistocene. According to the calibration performed, *A. monica* and *A. franciscana* would have diverged at different geologic times; the Late Pleistocene (0.13 Mya) and the Holocene (0.002 Mya), respectively. Therefore, it is necessary to highlight their specific status based on ecological and potential reproductive isolation (migrants are selected against, as demonstrated by Bowen [124]. Following our result, *Artemia franciscana* would have evolved more recently.

Artemia also consists of obligate parthenogenetic forms, independent of the *Artemia* species [116]. Although for several decades, parthenogenetic *Artemia* forms have been treated as *A. parthenogenetica*, Asem et al. [116] show it is an invalid binominal specific name, suggesting instead to consider them as "parthenogenetic lineage(s) of *Artemia*". The evolutionary relationship and origin(s) of *Artemia* parthenogenetic lineages was explored using electrophoretic markers by Abreu-Grobois and Beardmore [114] in American and Mediterranean species, including parthenogenetic lineages with different ploidy levels. However, as Asian species were not included, all parthenogenetic lineages were clustered in one major clade with Mediterranean *A. salina* being the sister clade. They concluded that: 1) the diploid parthenogenetic lineage has arisen from Mediterranean *A. salina*; 2) the tetraploid parthenogenetic lineage diverged from diploid parthenogenetic lineages; 3) the pentaploid parthenogenetic lineage originated from tetraploid parthenogenetic lineages, and; 4) the triploid parthenogenetic lineage could have arisen independently from diploid parthenogenetic lineages. Later, Beardmore and Abreu-Grobois [42] included the Asian species *A. urmiana* and revised their previous hypothesis, stating that parthenogenetic lineages arose from *A. urmiana*. Both studies introduced parthenogenetic lineages as a monophyletic group. Nevertheless, a comprehensive study based on four ploidy levels of parthenogens and using three mitochondrial (maternal) markers (*COI, 16S* and *12S*) revealed that parthenogenetic *Artemia* clustered in four distinct and well supported clades, each with different origins ([38], see also [18]). Our results also demonstrate that parthenogenetic *Artemia* lineages are a maternally polyphyletic group. Previously, it was suggested that diploid parthenogenetic lineages originated from *A. amati* ([17]; for more information see [49]) (*A. amati* was not described at that time [4]) and/or *A. urmiana* ([18, 38] see also [49]). Our mitogenome-based phylogenetic tree does not show a common ancestor between di-/triploid parthenogenetic lineages and *A. urmiana*. Thus, *A. urmiana* did not play a role in the origin of the diploid parthenogenetic lineage as previously suggested (see below). Our mitogenomic evidence shows that the common ancestor of *A. amati*/*A. tibetiana* (*ca.* 0.37 My, node M) and the common ancestor of diploid and triploid parthenogenetic lineages (*ca.* 0.07 Mya, node L) originated from a common historical ancestor (*ca.* 0.61 Mya, node K) in the Late Pleistocene. Thus, there is no direct maternal evolutionary link between *A. amati* and the diploid or triploid parthenogenetic lineages. We hypothesize that the origin of the diploid parthenogenetic lineage could be linked to mutational event(s) in the genome of the historical ancestor of diploid parthenogens. Regretfully, the historical correlate of the diploid parthenogenetic lineage is unclear.

Rode et al. [49] recognized two groups of diploid parthenogenetic *Artemia* ("diploid parthenogenetic *Artemia* with *A. urmiana* type mitochondria" and "diploid parthenogenetic *Artemia* with *Artemia* sp. Kazakhstan [later described as *A. amati*] type mitochondria") using a partial sequence (<700 bp) of *COI* haplotype network distribution. However, haplotype networks cannot reconstruct phylogenies (McFadden, per. com., 2022) or ancestral evolutionary relationships among taxa. Asem et al. [4] used three maternal markers (*COI*, *16S* and *12S*) to illustrate haplotype network distributions among Asian species. Using *16S* sequences, *A. tibetiana* was located between *A. urmiana* and *A. amati* (*Artemia* sp. Kazakhstan in ([49], for more information see 4], but in contrast, using a *12S* sequences haplotype network, *A. amati* was located between *A. urmiana* and *A. tibetiana*. Furthermore, *A. tibetiana* and *A. amati* have parallel positions in connection to *A. urmiana,* based on a *COI* haplotype network. The same problem can be found in multivariate analysis plots (PCoA, PCA, DA, etc.) using SSR/ISSR markers and morphological characters, where cluster position(s) can be changed with an increasing/decreasing number of studied groups. However, multivariant analysis plots cannot reconstruct ancestral evolutionary relationships and phylogenies. Both haplotype network distribution and multivariant analysis are useful bioinformatic tools to consider gene flow between taxa but are not reliable for phylogeny. Given that "diploid parthenogenetic *Artemia* with *A. urmiana* type mitochondria" [see [49]) was not analyzed in our study, its placement in the mitogenomic phylogeny is still open.

Generally, five hypotheses would explain the origin of the triploid parthenogenetic lineage: 1) fertilization of an unreduced ovum (secondary oocyte) from a diploid parthenogenetic *Artemia* by a sperm cell of *A. urmiana* ([18], see also [49]; 2) an unreduced *A. urmiana* ovum by sperm of a rare diploid parthenogen male [18]; 3) an unreduced *A. urmiana* ovum with *A. urmiana* sperm; 4) via polyspermy of a normal *A. urmiana* ovum, and; 5) via fertilization of two reduced nuclei (polar bodies) and a reduced ovum of a diploid parthenogen [38]. As discussed above, there is no common maternal ancestor between *A. urmiana* (and *A. amati*) and the triploid parthenogenetic lineage. Thus, an unreduced *A. urmiana* ovum (and an unreduced *A. amati* ovum) would not have had a maternal evolutionary function in the origin of the triploid parthenogenetic lineage. Following our mitogenomic phylogeny tree (see also [18]) and previous studies on SSR nuclear markers [49], triploid parthenogens could have originated through: 1) fusion of a normal ovum of diploid parthenogen with its two polar bodies 2) polyspermy of normal ovum of a diploid parthenogenetic *Artemia* via sperm of its own rare male(s), or; 3) fertilization of a diploid parthenogenetic *Artemia* unreduced ovum (secondary oocyte) with its rare male.

Consistent with previous studies [18, 38], our mitogenomic phylogeny demonstrates that *A. sinica* shares a historical maternal ancestor (*ca.* 0.96 Mya, in Early Pleistocene) with the common ancestor (*ca.* 0.05 Mya, Late Pleistocene) of tetraploid and pentaploid parthenogenetic lineages.

Rode et al. [49] proposed that tetraploid parthenogens could have originated by hybridization between *A. sinica* (maternal origin) and a rare male of a diploid parthenogenetic lineage (paternal origin). In contrast to Rode et al. [49], who referred to the historical hybridization event in East Siberia using a single sequence named "*A. sinica* (?)" (LC195586; [125]), we suggest that hybridization between *A. sinica* and a rare male of a diploid parthenogenetic *Artemia* should have occurred in East Asia. Biogeographically, *A. sinica* only occurs in East Asia, and there is no taxonomic evidence that LC195586 (TU13), obtained from a batch including two females from Lake Dus-Kholin in Siberia (see [125]), belongs to a bisexual population and/or *A. sinica*. Additionally, the sequence of TU13 most likely is a tetraploid (or pentaploid) parthenogenetic lineage, whereas the sequence quality and taxonomic status of specimens studied by Naganawa and Mura [125] are problematic and questionable (see [4, 34, 61, 63]). It is most unlikely that TU13 could be an introduced exotic specimen of *A. sinica*.

Asem et al. [38] suggested that the pentaploid parthenogenetic lineage may have evolved from an allopolyploid (hybridization) of *A. sinica* sperm and a tetraploid ovum or autopolyploid. The lack of gene exchange between the nuclear genes of *A. sinica* and pentaploid parthenogens (see [49]), cast doubts on the role of *A. sinica* in the origin of the pentaploid parthenogenetic lineage. Therefore, the autopolyploid or allopolyploid (historical hybridization with the paternal source of *A. sorgeloosi* and/or *A. tibetiana*) is most likely the origin of the pentaploid parthenogenetic lineage (see also [49, 4]).

Our mitogenomic study clarifies the phylogenetic tree topography controversies of previous studies. For example, the initial allozyme study [42] put the New World species together in a major clade, with *A. salina* and Asian species in another. Later, studies using the partial mitochondrial *COI* put either the New World *A. persimilis* [18] or the Mediterranean *A. salina* in a basal clade [21]. However, an abnormal phylogenetic tree using *COI* by Muñoz et al.'s [16] had the New World *A. franciscana* between *A. sinica* and other Asian members.

Later trees based on the nuclear *ITSI* marker showed *A. salina* between the New World *A. franciscana* (*A. monica* not analyzed) and South American *A. persimilis* [18, 21, 38]. According to our results, the maternal ancestral clade of *Artemia* split into ancestral lineages of *A. persimilis* and *A. salina* in *ca.* 33.97 Mya in the Early Oligocene/Late Eocene, which should have originated in the Mediterranean area or South America. Although the Mediterranean area can be assumed as one of the possible geological origins of *Artemia*, the proposition of the Mediterranean area as the origin of *Artemia* divergence, as suggested by Beardmore and Abreu-Grobois [42], due to the extreme salinity rise there, now seems debatable. The Messinian salinity crisis in the Mediterranean basin occurred 6–5.3 Mya [126]. Therefore, this event cannot be referred to as the cause of *Artemia* diversification, which, according to our results, occurred *ca.* 33.97 Mya. Even so, the Messinian salinity crisis has probably played a role in the expansion of *A. salina* in the Mediterranean region.

Artemia diversification in the New World continued from the ancestral lineage of *A. salina* in the Mediterranean area via a common ancestor of *A. monica* and *A. franciscana* (*ca.* 21.10 Mya), whereas Asian *Artemia* diverged through a maternal ancestor lineage of *A. sinica* from East Asia (*ca.* 14.27 Mya). East Asia was the maternal origin of the tetraploid (*ca.* 0.1 Mya) and pentaploid parthenogenetic lineages (*ca.* 0.002 Mya). The Tibetan Plateau was the dispersal bridge for *Artemia* from East to West Asia [for the origin of *A. urmiana*; see [50, 127] via the maternal ancestor lineage of *A. sorgeloosi* in *ca.* 4.85 Mya. The Tibetan Plateau and Central Asia are recent scenarios of *Artemia* divergence (*A. tibetiana* and *A. amati*, respectively) through the maternal ancestor lineage of *A. urmiana,* which occurred *ca.* 1.3 Mya. Although the geologic origin(s) of diploid and triploid parthenogenetic lineages are unclear, their origin(s) should be in West and/or Central Asia.

Conclusion

The brine shrimp *Artemia* is a paradigmatic crustacean genus adapted to the variable hypersaline conditions, with sexual species and parthenogenetic lineages, whose evolutionary relationships and divergence times are updated by this study based on the whole mitochondrial genome. Relevant conclusions are:

1. Complete mitochondrial genomes (mitogenomes) can provide a clear phylogeny relationship and clarify common ancestor(s).
2. The *Artemia* diversification occurred from the ancestral lineages of *A. salina* in the Mediterranean area and *A. persimilis* in South America (*ca.* 33.97 Mya), followed by the ancestral lineage of “North America and Asia” (*ca.* 26.32 Mya). North America *Artemia* diverged in *ca.* 0.44 Mya and Asian *Artemia* in East Asia in *ca.* 14.27 Mya. East Asia was the maternal origin of the tetraploid (*ca.* 0.1 Mya) and pentaploid parthenogenetic lineages (*ca.* 0.002 Mya). Geological origins of diploid (*ca.* 0.0005 Mya) and triploid (*ca.* 0.007 Mus) lineages probably developed in West and/or Central Asia.
3. Asian *Artemia* originated from multiple ancestors that diverged in different geologic periods. Therefore, unlike previous studies, Asian species cannot be considered “species complex.”
4. The mitogenomic phylogenetic tree shows no direct association between maternal sources of *A. amati* and the diploid parthenogenetic lineage from Gahai Lake (“diploid parthenogenetic *Artemia* with *Artemia* sp. Kazakhstan type mitochondria” as previously reported [49]). They are, however, linked via three noncommon ancestors in our analysis. Therefore, maternal sources of diploid parthenogenetic *Artemia* cannot be traced back to the mitochondria of *A. amati*, which has its own independent mitogenome evolutionary origin. Moreover, our findings exhibit an identical evolutionary status for *A. amati* and *A. tibetiana* in relation to diploid parthenogenetic *Artemia*.
5. The taxonomic status of *A. monica* and *A. franciscana* has been controversial; however, in addition to the evidence of ecological and reproductive isolation, differentiation in tRNAs secondary structure, nucleotide compositions, RSCU, and especially intraspecific divergence time and geologic occurrence periods, *A. monica* and *A. franciscana* are demonstrably two distinct species (see also [23]).
6. Our case study shows that parthenogenetic *Artemia* is a maternally polyphyletic group, and that the tetraploid lineage divided in a different geologic time (Late Pleistocene *vs.* Holocene). Based on zoological species concepts and on *Artemia* polyphyletic evolutionary relationships, parthenogenetic lineages cannot be referred to as the binominal specific nomen “*Artemiaparthenogenetica*”. The parthenogenetic lineages originated from several historical hybridization events, including crosses and backcrosses within Asian species.
7. Asian and North American *Artemia* are the most recently diversified taxa, and the value of genetic distance cannot be a reliable scale for species delimitation.

Supplementary Information

The online version contains supplementary material available at https://doi.org/10.1186/s12864-025-11391-6.

Supplementary Material 1

Acknowledgements
The authors thank Dr. Shi-Chun Sun (Ocean University of China, China) and Dr. Gilbert Van Stappen (Gent University, Belgium) for preparing the *Artemia* eggs. The help of Miss Bo Wang (Haina Tropical Ocean University, China) is highly appreciated. For valuable advice, the authors are grateful to Dr. Lenormand (University of Montpellier, France) Dr. Rode (University of Montpellier, France). A.A. acknowledges Dr. Shi-Chun Sun for use of his laboratory facilities to culture examined samples of this study during his Post-Doc (2015-2017) in Ocean University of China.

Authors' contributions
A.A.: experimental design, data analysis, draft manuscript preparation. C.Y.: data analysis, draft manuscript preparation, funding. S.D.: data analysis, experimental design, manuscript revision. E.M.: data analysis. X.L.: data analysis. C.S.: Collation of data, data analysis, funding. F.H. Supervision, experimental design, manuscript revision. D.C.R.: Supervision, experimental design, manuscript revision. G.G.: Supervision, experimental design, manuscript revision. All authors reviewed the results and approved the final version of the manuscript.

Funding
This study has been supported by the National Key R&D Program of China (2024YFD2401804), Key Research and Development Project of Hainan Province in 2022, Research and Application of High Quality Breeding Technologies for striped scat (Selenotoca multifasciata) and Seedlings (Fund No.ZDYF2022XDNY331) and Research Project of Chengde Medical University (Grant No. 202419).

Data Availability
The sequence data (OR423222; OR423223; OP800906; OP805358; OR423229; OR423219; OR423218; OR423228; OR423226; OR423227; OR423224; OR423225; OR423220; OR423221; OR423214; OR423215; OR423216; OR423217; OR423213; OP805359; OP830835; OP830836) of this study are openly available in GenBank NCBI at https://www.ncbi.nlm.nih.gov/.

Declarations

Ethics approval and consent to participate
The authors have complied with all ethical standards required for conducting this research. Consents and approvals are not applicable to this research.

Consent for publication
Not applicable.

Competing interests
The authors declare no competing interests.

Author details
[1]College of Fisheries and Life Sciences, Hainan Tropical Ocean University, Sanya 572000, China. [2]Department of Applied Animal Science and Welfare, Swedish University of Agricultural Sciences, Aquakultur, Sweden. [3]Faculty of Chemical Engineering, Kunming University of Science and Technology, Kunming, Yunnan 650500, China. [4]Department of Biology, Chengde Medical University, Chengde 067000, China. [5]Instituto de Acuicultura de Torre de La Sal (IATS, CSIC), Ribera de Cabanes (Castellón) 12595, Spain. [6]GRDA Scenic Rivers & Watershed Research Laboratory, Northeastern State University, 611 N Grand Ave, Tahlequah, OK 74464-2302, USA. [7]Departamento de Ciencias Biológicas y Biodiversidad, Universidad de Los Lagos, Osorno 5290000, Chile.

Received: 30 October 2024 Accepted: 20 February 2025
Published online: 10 March 2025

References

1. Gajardo G, Beardmore JA. The brine shrimp *Artemia*: adapted to critical life conditions. Front physiol. 2012;3:185. https://doi.org/10.3389/fphys.2012.00185.
2. Gajardo G, Abatzopoulos TJ, Kappas I, Beardmore JA. Evolution and Speciation. In: Abatzopoulos TJ, Beardmore JA, Clegg JS, Sorgeloos P, editors. *Artemia* Basic and Applied Biology. Dordrecht: Kluwer Academic Publishers; 2002. p. 225–50.
3. Rogers DC. A conceptual model for anostracan biogeography. J Crustac Biol. 2015;35(5):686–99. https://doi.org/10.1163/1937240X-00002369.
4. Asem A, Yang C, Eimanifar A, Hontoria F, Varó I, Mahmoudi F, Fu C, Shen C, Rastegar-Pouyani N, Wang P, Li W, Yao L, Meng X, Dan Y, Rogers C, Gajardo G. Phylogenetic analysis of problematic Asian species of *Artemia* Leach, 1819 (Crustacea, Anostraca), with the descriptions of two new species. J Crustac Biol. 2023;43(1):1–25. https://doi.org/10.1093/jcbiol/ruad002.
5. Asem A, Yang C, Mahmoudi F, Chen S, Long B, Wang B, Fu C, Hontoria F, Rogers DC, Gajardo G. Tibetan *Artemia* (Crustacea: Anostraca) mitogenomic biodiversity and population demographics. Zool J Linn Soc. 2024;201(1):32–56. https://doi.org/10.1093/zoolinnean/zlad114.
6. Amat F. Diferenciacion y distribucion de las poblaciones de *Artemia* (crustaceo, branquiopodo) de Espana, 2: Incidencia de la salinidad ambiental sobre la morfologia y el desarrollo. Inv Pesq. 1980;44:485–503.
7. El-Bermawi N, Baxevanis AD, Abatzopoulos TJ, Van Stappen G, Sorgeloos P. Salinity effects on survival, growth and morphometry of four Egyptian *Artemia* populations (International Study on *Artemia*. LXVII). Hydrobiologia. 2004;523(1–3):175–188. https://doi.org/10.1023/B:HYDR.0000033124.49676.5c.
8. Litvinenko LI, Boyko EG. The morphological characteristics of *Artemia* shrimps from Siberian populations. Inland Water Biol. 2008;1(1):37–45. https://doi.org/10.1007/s12212-008-1007-0.
9. Ben Naceur H, Jenhani ABR, Romdhane MS. In situ study of adult *Artemia salina* morphometry and its relationship to the physicochemical water parameters in the saltwork of Sahline (Tunisia). Int J Oceanogr Hydrobio. 2011;40(4):44–51. https://doi.org/10.2478/s13545-011-0040-5.
10. Ben Naceur H, Jenhani ABR, Romdhane MS. Influence of environmental factors on the life cycle and morphology of *Artemia salina* (Crustacea: Anostraca) in Sabkhet El Adhibet (SE Tunisia). Biol Lett. 2011;48(1):67–83. https://doi.org/10.2478/v10120-011-0008-6.
11. Ben Naceur H, Jenhani ABR, Romdhane MS. Impacts of salinity, temperature, and pH on the morphology of *Artemia salina* (Branchiopoda: Anostraca) from Tunisia. Zool Stud. 2012;51(3–4):453–62.
12. Hebert PD, Remigio EA, Colbourne JK, Taylor DJ, Wilson CC. Accelerated molecular evolution in halophilic crustaceans. Evolution. 2002;56(5):909–26. https://doi.org/10.1111/j.0014-3820.2002.tb01404.x.
13. Tong C, Li M. Genomic signature of accelerated evolution in a saline-alkaline lake-dwelling Schizothoracine fish. Int J Biol Macromol. 2020;149:341–7. https://doi.org/10.1016/j.ijbiomac.2020.01.207.
14. Wurtsbaugh WA, Miller C, Null SE, DeRose RJ, Wilcock P, Hahnenberger M, Howe F, Moore J. Decline of the world's saline lakes. Nat Geosci. 2017;10:816–21. https://doi.org/10.1038/NGEO3052.
15. Gajardo G, Redón S. Andean hypersaline lakes in the Atacama Desert, northern Chile: Between lithium exploitation and unique biodiversity conservation. Conserv sci pract. 2019;1: e94. https://doi.org/10.1111/csp2.94.
16. Muñoz J, Gómez A, Green AJ, Figuerola J, Amat F, Rico C. Phylogeography and local endemism of the native Mediterranean brine shrimp *Artemia salina* (Branchiopoda: Anostraca). Mol Ecol. 2008;17(13):3160–77. https://doi.org/10.1111/j.1365-294x.2008.03818.x.
17. Muñoz J, Gomez A, Green AJ, Figuerola J, Amat F, Rico C. Evolutionary origin and phylogeography of the diploid obligate parthenogen *Artemia parthenogenetica* (Branchiopoda: Anostraca). PLoS ONE. 2010;5: e11932. https://doi.org/10.1371/journal.pone.0011932.
18. Maniatsi S, Baxevanis AD, Kappas I, Deligiannidis P, Triantafyllidis A, Papakostas S, Bougiouklis D, Abatzopoulos TJ. Is polyploidy a persevering accident or an adaptive evolutionary pattern? The case of the brine shrimp *Artemia*. Mol Phylogenet Evol. 2011;58(2):353–64. https://doi.org/10.1016/j.ympev.2010.11.029.

19. Maccari M, Amat F, Gómez A. Origin and genetic diversity of diploid parthenogenetic *Artemia* in Eurasia. PLoS ONE. 2013;8: e83348. https://doi.org/10.1371/journal.pone.0083348.
20. Baxevanis AD, Maniatsi S, Kouroupis D, Marathiotis K, Kappas I, Kaiser H, Abatzopoulos TJ. Genetic identification of South African *Artemia* species: invasion, replacement and co-occurrence. J Mar Biol Assoc UK. 2014;94(4):775–85. https://doi.org/10.1017/S0025315414000083.
21. Eimanifar A, Van Stappen G, Marden B, Wink M. *Artemia* biodiversity in Asia with the focus on the phylogeography of the introduced American species *Artemia franciscana* Kellogg, 1906. Mol Phylogenet Evol. 2014;79:392–403. https://doi.org/10.1016/j.ympev.2014.06.027.
22. Eimanifar A, Van Stappen G, Wink M. Geographical distribution and evolutionary divergence times of Asian populations of the brine shrimp *Artemia* (Crustacea, Anostraca). Zool J Linn Soc. 2015;174(3):447–58. https://doi.org/10.1111/zoj.12242.
23. Asem A, Gajardo G, Rogers DC, Sorgeloos P. The taxonomic status of *Artemia monica* Verrill, 1869 (Crustacea: Anostraca). Zool J Linn Soc. 2024;201(3):1–5. https://doi.org/10.1093/zoolinnean/zlae088.
24. Asem A, Eimanifar A, Rastegar-Pouyani N, Hontoria F, De Vos S, Van Stappen G, Sun SC. An overview on the nomenclatural and phylogenetic problems of native Asian brine shrimps of the genus *Artemia* Leach, 1819 (Crustacea: Anostraca). Zookeys. 2020;902:1–15. https://doi.org/10.3897/2Fzookeys.902.34593.
25. Hontoria F, Amat F. Morphological characterization of adult *Artemia* (Crustacea, Branchiopoda) from different geographical origin. Mediterranean populations J Plankton Res. 1992;14(7):949–59. https://doi.org/10.1093/plankt/14.7.949.
26. Hontoria F, Amat F. Morphological characterization of adult *Artemia* (Crustacea, Branchiopoda) from different geographical origins. American populations J Plankton Res. 1992;14(10):1461–71. https://doi.org/10.1093/plankt/14.10.1461.
27. Gajardo G, Crespo J, Triantafyllidis A, Tzika A, Baxevanis AD, Kappas I, Abatzopoulos TJ. Species identification of Chilean *Artemia* populations based on mitochondrial DNA RFLP analysis. J Biogeogr. 2004;31(4):547–55. https://doi.org/10.1111/j.1365-2699.2003.01046.x.
28. Amat F. Differentiation in *Artemia* strains from Spain. In: Persoone G, Sorgeloos P, Roels O., Jaspers E. (Eds.), The Brine Shrimp *Artemia* (Vol. 1). Universa Press, Wetteren, 1980. p. 19–39.
29. Amat F, Barata C, Hontoria F. A Mediterranean origin for the Veldrif (South Africa) *Artemia* Leach population. J Biogeogr. 1995;22(1):49–59. https://doi.org/10.2307/2846072.
30. Triantaphyllidis GV, Criel GRJ, Abatzopoulos TJ, Sorgeloos P. International study on *Artemia*. LIV. Morphological study on *Artemia* with emphasis to Old World strains. II. Parthenogenetic populations. Hydrobiologia. 1997;357(1):155–163. https://doi.org/10.1023/A:1003195021939.
31. Sun Y, Zhong Y, Song W, Zhang R, Chen R. Detection of genetic relationships among four *Artemia* species using randomly amplified polymorphic DNA (RAPD). Int J Salt Lake Res. 1999;8(2):139–47. https://doi.org/10.1023/A:1009039815660.
32. Hontoria F, Redón S, Maccari M, Varó I, Navarro JC, Ballell L, Amat F. A revision of *Artemia* biodiversity in Macaronesia. Aquat Biosyst. 2012;8:25. https://doi.org/10.1186/2046-9063-8-25.
33. Maccari M, Gómez A, Hontoria F, Amat F. Functional rare males in diploid parthenogenetic *Artemia*. J Evol Biol. 2013;26(9):1934–48. https://doi.org/10.1111/jeb.12191.
34. Eimanifar A, Asem A, Wang P-Z, Li W, Wink M. Using ISSR Genomic Fingerprinting to Study the Genetic Differentiation of *Artemia* Leach, 1819 (Crustacea: Anostraca) from Iran and Neighbor Regions with the Focus on the Invasive American *Artemia franciscana*. Diversity. 2020;12(4):132. https://doi.org/10.3390/d12040132.
35. Asem A, Sun SC. Biometric characterization of Chinese parthenogenetic *Artemia* (Crustacea: Anostraca) cysts, focusing on its relationship with ploidy and habitat altitude. North-west J Zool. 2014;10(1):149–57.
36. Asem A, Sun SC. SEM study of diversity in the cyst surface topography of nine parthenogenetic *Artemia* populations from China. Microsc Res Tech. 2014;77(12):1005–14. https://doi.org/10.1002/jemt.22429.
37. Asem A, Sun SC. Morphological differentiation of seven parthenogenetic *Artemia* (Crustacea: Branchiopoda) populations from China, with special emphasis on ploidy degrees. Microsc Res Tech. 2016;79(4):258–66. https://doi.org/10.1002/jemt.22625.
38. Asem A, Eimanifar A, Sun SC. Genetic variation and evolutionary origins of parthenogenetic *Artemia* (Crustacea: Anostraca) with different ploidies. Zool Scr. 2016;45(4):421–36. https://doi.org/10.1111/zsc.12162.
39. Timms BV. An identification guide to the brine shrimps (Crustacea: Anostraca: Artemiina) of Australia. Museum Victoria. Sci Rep. 2012;16:1–36. https://doi.org/10.24199/j.mvsr.2012.16.
40. Timms BV. A review of the biology of Australian halophilic anostracans (Branchiopoda: Anostraca). J. Biol. Res. Thessalon. 2014;21:21. https://doi.org/10.1186/2F2241-5793-21-21.
41. Rogers DC, Timms BV. Anostracan (Crustacea: Branchiopoda) zoogeography III. Australian bioregions. Zootaxa. 2014;3881(5):453–87. https://doi.org/10.11646/zootaxa.3881.5.3.
42. Beardmore JA, Abreu-Grobois FA. Taxonomy and Evolution in the Brine Shrimp *Artemia*. In: Oxford GS, Rollinson D, editors. Protein Polymorphism: Adaptive and Taxonomic Significance. London: Academic Press; 1983. p. 153–64.
43. Triantaphyllidis GV, Criel GRJ, Abatzopoulos TJ, Sorgeloos P. International study on *Artemia*. LIII. Morphological study of *Artemia* with emphasis to Old World strains. I. Bisexual populations. Hydrobiologia. 1997;357(1):139–153. https://doi.org/10.1023/A:1003190905100.
44. Gajardo G, Colihueque N, Parraguez M, Sorgeloos P. International Study on *Artemia* LVIII. Morphologic differentiation and reproductive isolation of *Artemia* populations from South America. Int J Salt Lake Res. 1998;7(2):133–151 https://doi.org/10.1023/A:1009057306033.
45. Baxevanis AD, Triantaphyllidis GV, Kappas I, Triantafyllidis A, Triantaphyllidis CD, Abatzopoulos TJ. Evolutionary assessment of *Artemia tibetiana* (Crustacea, Anostraca) based on morphometry and 16S rRNA RFLP analysis. J Zool Syst Evol. 2005;43:189–98. https://doi.org/10.1111/j.1439-0469.2005.00309.x.
46. Baxevanis AD, Kappas I, Abatzopoulos TJ. Molecular phylogenetics and asexuality in the brine shrimp *Artemia*. Mol Phylogenet Evol. 2006;40(3):724–38. https://doi.org/10.1016/j.ympev.2006.04.010.
47. Kappas I, Baxevanis AD, Maniatsi S, Abatzopoulos TJ. Porous genomes and species integrity in the branchiopod *Artemia*. Mol Phylogenet Evol. 2009;52(1):192–204. https://doi.org/10.1016/j.ympev.2009.03.012.
48. Nougue O, Flaven E, Jabbour-Zahab R, Rode NO, Dubois M, Lenormand T. Characterization of nine new polymorphic microsatellite markers in *Artemia parthenogenetica*. Biochem Syst Ecol. 2015;58:59–63. https://doi.org/10.1016/j.bse.2014.09.024.
49. Rode NO, Jabbour-Zahab R, Boyer L, Flaven É, Hontoria F, Van Stappen G, Dufresne F, Haag C, Lenormand T. The Origin of Asexual Brine Shrimps. Am Nat. 2022;200(2):E52–76. https://doi.org/10.1086/720268.
50. Abatzopoulos TJ, Amat F, Baxevanis AD, Belmonte G, Hontoria F, Maniatsi S, Moscatello S, Mura G, Shadrin NV. Updating geographic distribution of *Artemia urmiana* Günther, 1890 (Branchiopoda: Anostraca) in Europe: An integrated and interdisciplinary approach. Int Rev Hydrobiol. 2009;94(5):560–79. https://doi.org/10.1002/iroh.200911147.
51. Duchêne S, Archer FI, Vilstrup J, Caballero S, Morin PA. Mitogenome Phylogenetics: The Impact of Using Single Regions and Partitioning Schemes on Topology, Substitution Rate and Divergence Time Estimation. PLoS ONE. 2011;6(11): e27138. https://doi.org/10.1371/journal.pone.0027138.
52. Morón-López J, Vergara K, Sato M, Gajardo G, Ueki S. Intraspecies variation of the mitochondrial genome: An evaluation for phylogenetic approaches based on the conventional choices of genes and segments on mitogenome. PLoS ONE. 2022;17(8): e0273330. https://doi.org/10.1371/journal.pone.0273330.
53. Boore JL. Animal mitochondrial genomes. Nucleic Acids Res. 1999;27(8):1767–80. https://doi.org/10.1093/nar/27.8.1767.
54. Miller W, Drautz DI, Janecka JE, Lesk AM, Ratan A, Tomsho LP, Packard M, Zhang Y, McClellan LR, Qi J, Zhao F, Gilbert MT, Dalén L, Arsuaga JL, Ericson PG, Huson DH, Helgen KM, Murphy WJ, Götherström A, Schuster SC. The mitochondrial genome sequence of the Tasmanian tiger (*Thylacinus cynocephalus*). Genome Res. 2009;19(2):213–20. http://www.genome.org/cgi/doi/https://doi.org/10.1101/gr.082628.108.
55. Bronstein O, Kroh A, Haring E. Mind the gap! The mitochondrial control region and its power as a phylogenetic marker in echinoids. BMC Ecol Evol. 2018;18:80. https://doi.org/10.1186/s12862-018-1198-x.

56. Dong Z, Wang Y, Li C, Li L, Men X. Mitochondrial DNA as a molecular marker in insect ecology: Current status and future prospects. Ann Entomol Soc Am. 2021;114(4):470–6. https://doi.org/10.1093/aesa/saab020.
57. Schwartz JH. Evolution, systematics, and the unnatural history of mitochondrial DNA. Mitochondrial DNA Part A. 2021;32(4):126–51. https://doi.org/10.1080/24701394.2021.1899165.
58. Hill GE. Genetic hitchhiking, mitonuclear coadaptation, and the origins of mt DNA barcode gaps. Ecol Evol. 2020;10(17):9048–59. https://doi.org/10.1002/ece3.6640.
59. Wang X, Pei J, Bao P, Cao M, Guo S, Song R, Song W, Liang C, Yan P, Guo X. Mitogenomic diversity and phylogeny analysis of yak (*Bos grunniens*). BMC Genomics. 2021;22:325. https://doi.org/10.1186/s12864-021-07650-x.
60. De Vos S, Rombauts S, Coussement L, Dermauw W, Vuylsteke M, Sorgeloos P, Clegg JS, Nambu Z, Van Nieuwerburgh F, Norouzitallab P, Van Leeuwen T, De Meyer T, Van Stappen G, Van de Peer Y, Bossier P. The genome of the extremophile *Artemia* provides insight into strategies to cope with extreme environments. BMC Genomics. 2021;22:635. https://doi.org/10.1186/s12864-021-07937-z.
61. Asem A, Eimanifar A, Li W, Shen CY, Shikhsarmast FM, Dan YT, Lu H, Zhou Y, Chen Y, Wang P, Wink M. Reanalysis and revision of the complete mitochondrial genome of *Artemia urmiana* Günther, 1899 (Crustacea: Anostraca). Diversity. 2021;13(1):14. https://doi.org/10.3390/d13010014.
62. Saleem CM, Asem A, Sun SC. The incidence of rare males in seven parthenogenetic *Artemia* (Crustacea: Anostraca) populations. Turk J Zool. 2017;41(1):138–43. https://doi.org/10.3906/zoo-1512-67.
63. Asem A, Fu C, Yang N, Eimanifar A, Cao Y, Wang P, Shen C. Validation of two novel primers for the promising amplification of the mitogenomic Cytochrome c Oxidase subunit I (*COI*) barcoding region in *Artemia* aff. *sinica* (Branchiopoda, Anostraca). Crustaceana. 2022;95(5–6):585–592. https://doi.org/10.1163/15685403-bja10207.
64. Asem A, Li W, Wang PZ, Eimanifar A, Shen CY, De Vos S, Van Stappen G. The complete mitochondrial genome of *Artemia sinica* Cai, 1989 (Crustacea: Anostraca) using next-generation sequencing. Mitochondrial DNA B Resour. 2019;4(1):746–7. https://doi.org/10.1080/23802359.2019.1565933.
65. Andrews S. FastQC: A Quality Control Tool for High Throughput Sequence Data. (04–10–18: Version 0.11.8 Released). http://www.bioinformatics.babraham.ac.uk/projects/fastqc, 2010. (accessed on 11 November 2010).
66. Perez ML, Valverde JR, Batuecas B, Amat F, Marco R, Garesse R. Speciation in the *Artemia* genus: mitochondrial DNA analysis of bisexual and parthenogenetic brine shrimps. J Mol Evol. 1994;38(2):156–68. https://doi.org/10.1007/bf00166162.
67. Langmead B, Salzberg S. Fast gapped-read alignment with Bowtie 2. Nat Methods. 2012;9:357–9. https://doi.org/10.1038/nmeth.1923.
68. Kearse M, Moir R, Wilson A, Stones-Havas S, Cheung M, Sturrock S, Buxton S, Cooper A, Markowitz S, Duran C, Thierer T, Ashton B, Meintjes P, Drummond A. Geneious Basic: An integrated and extendable desktop software platform for the organization and analysis of sequence data. Bioinformatics. 2012;28(2):1647–9. https://doi.org/10.1093/bioinformatics/bts199.
69. Zuker M. Mfold web server for nucleic acid folding and hybridization prediction. Nucleic Acids Res. 2003;31(13):3406–15. https://doi.org/10.1093/nar/gkg595.
70. Hall TA. BioEdit: a user-friendly biological sequence alignment editor and analysis program for Windows 95/98/NT. Nucleic Acids Symp Ser. 1999;41:95–8.
71. Xia X. DAMBE7: New and improved tools for data analysis in molecular biology and evolution. Mol Biol Evol. 2018;35(6):1550–2. https://doi.org/10.1093/molbev/msy073.
72. Perna NT, Kocher TD. Patterns of nucleotide composition at fourfold degenerate sites of animal mitochondrial genomes. J Mol Evol. 1995;41(3):353–8. https://doi.org/10.1007/BF00186547.
73. Kumar S, Stecher G, Li M, Knyaz C, Tamura K. MEGA X: Molecular evolutionary genetics analysis across computing platforms. Mol Biol Evol. 2018;35(6):1547–9. https://doi.org/10.1093/molbev/msy096.
74. Srivathsan A, Meier R. On the inappropriate use of Kimura-2-parameter (K2P) divergences in the DNA-barcoding literature. Cladistics. 2012;28(2):190–4. https://doi.org/10.1111/j.1096-0031.2011.00370.x.
75. Miller MA, Pfeiffer W, Schwartz T. Creating the CIPRES Science Gateway for inference of large phylogenetic trees, In: Proceedings of the Gateway Computing Environments Workshop (GCE), 14 Nov. 2010. New Orleans, LA, USA. 2010. p. 1–8.
76. Tladi M, Dalu T, Rogers DC, Nyamukondiwa C, Parbhu SP, Teske P, Emami-Khoyi A, Wasserman RJ. The complete mitogenome of the fairy shrimp *Streptocephalus cafer* (Lovén, 1847) (Crustacea: Branchiopoda: Anostraca) from an ephemeral pond in Botswana, southern Africa. Mitochondrial DNA B Resour. 2020;5(1):623–5. https://doi.org/10.1080/23802359.2019.1711222.
77. Nylander JAA. MrModeltest v2. Program distributed by the author. Evolutionary Biology Centre: Uppsala University, Uppsala, Sweden; 2004.
78. Rambaut A. FigTree (version 1.4.0) http://tree.bio.ed.ac.uk/software/figtree/ 2012. (accessed 24 January 2024).
79. Hillis DM, Bull JJ. An empirical test of bootstrapping as a method for assessing confidence in phylogenetic analysis. Syst Biol. 1993;42(2):182–92. https://doi.org/10.2307/2992540.
80. Alfaro ME, Zoller S, Lutzoni F. Bayes or bootstrap? A simulation study comparing the performance of Bayesian Markov chain Monte Carlo sampling and bootstrapping in assessing phylogenetic confidence. Mol Biol Evol. 2003;20(2):255–66. https://doi.org/10.1093/molbev/msg028.
81. Siddall ME, Whiting MF. Long-branch abstractions. Cladistics. 1999;15(1):9–24. https://doi.org/10.1111/j.1096-0031.1999.tb00391.x.
82. Bergsten JA. review of long-branch attraction. Cladistics. 2005;21(2):163–93. https://doi.org/10.1111/j.1096-0031.2005.00059.x.
83. O'Connor T, Sundberg K, Carroll H, Clement M, Snell Q. Analysis of long branch extraction and long branch shortening. BMC Genomics. 2010;11(Suppl 2):S14. https://doi.org/10.1186/1471-2164-11-S2-S14.
84. Manzi V, Lugli S, Roveri M, Pierre FD, Gennari R, Lozar F, Natalicchio M, Schreiber BC, Taviani M, Turco E. The Messinian salinity crisis in Cyprus: a further step towards a new stratigraphic framework for Eastern Mediterranean. Basin Res. 2016;28(2):207–36. https://doi.org/10.1111/bre.12107.
85. Mura G, Hadjistephanou N. First records *of Branchinella spinosa,* Milne Edwards (Crustacea, Anostraca) in Cyprus. Riv Idrobiol. 1987;26(1–3):111–5.
86. Karagianni A, Stamou G, Katsiapi M, Polykarpou P, Dörflinger G, Michaloudi E. Zooplankton communities in Mediterranean temporary lakes: the case of saline lakes in Cyprus. Int J Limnol. 2018;54:14. https://doi.org/10.1051/limn/2018007.
87. Kotov AA, Taylor DJ. Mesozoic fossils (> 145 mya) suggest the antiquity of the subgenera of *Daphnia* and their coevolution with chaoborid predators. BMC Ecol Evol. 2011;11:129. https://doi.org/10.1186/1471-2148-11-129.
88. Suchard MA, Lemey P, Baele G, Ayres DL, Drummond AJ, Rambaut A. Bayesian phylogenetic and phylodynamic data integration using BEAST 1.10. Virus Ecolo. 2018;4(1):vey016. https://doi.org/10.1093/ve/vey016.
89. Yule GU. A mathematical theory of evolution, based on the conclusions of Dr. J. C. Willis, F.R.S. Philos Trans R Soc B. 1925;213(402–410):21–87. https://doi.org/10.1098/rstb.1925.0002.
90. Gernhard T. The conditioned reconstructed process. J Theor Biol. 2008;253(4):769–78. https://doi.org/10.1016/j.jtbi.2008.04.005.
91. Sigvardt ZM, Olesen J, Rogers DC, Timms B, Mlambo M, Rabet N, Palero F. Multilocus phylogenetics of smooth clam shrimps (Branchiopoda, Laevicaudata). Zool Scr. 2021;50(6):795–811. https://doi.org/10.1111/zsc.12505.
92. Minin V, Suchard M. Counting labeled transitions in continuous time Markov models of evolution. J Math Biol. 2008;56:391–412. https://doi.org/10.1007/s00285-007-0120-8.
93. Rambaut A, Drummond AJ, Xie D, Baele G, Suchard MA. Posterior summarisation in Bayesian phylogenetics using Tracer 1.7. Syst Biol. 2018;67(5):901–904. https://doi.org/10.1093/sysbio/syy032.
94. Shao T, Wang W, Duan M, Pan J, Xin Z, Liu B, Zhou F, Wang G. Application of Bayesian phylogenetic inference modelling for evolutionary genetic analysis and dynamic changes in 2019-nCoV. Brief Bioinform. 2021;22(2):896–904. https://doi.org/10.1093/bib/bbaa154.
95. Nara L, Cremer MJ, Farro APC, Colosio AC, Barbosa LA, Bertozzi CP, Secchi ER, Pagliani B, Costa-Urrutia P, Gariboldi MC, Lazoski C, Cunha

HA. Phylogeography of the Endangered Franciscana Dolphin: Timing and Geological Setting of the Evolution of Populations. J Mamm Evol. 2022;29:609–25. https://doi.org/10.1007/s10914-022-09607-7.

96. Luchetti A, Forni G, Skaist AM, Wheelan SJ, Mantovani B. Mitochondrial genome diversity and evolution in Branchiopoda (Crustacea). Zool Lett. 2019;5:15. https://doi.org/10.1186/s40851-019-0131-5.
97. Geng X, Cheng R, Xiang T, Deng B, Wang Y, Deng D, Zhang H. The complete mitochondrial genome of the Chinese *Daphnia pulex* (Cladocera, Daphniidae). Zookeys. 2016;615:47–60. https://doi.org/10.3897/2Fzookeys.615.8581.
98. Coskun PE, Ruiz-Pesini E, Wallace DC. Control region mtDNA variants: Longevity, climatic adaptation, and a forensic conundrum. PNAS. 2003;100(5):2174–6. https://doi.org/10.1073/pnas.0630589100.
99. Podsiadlowski L, Carapelli A, Nardi F, Dallai R, Koch M, Boore JL, Frati F. The mitochondrial genomes *of Campodea fragilis* and *Campodea lubbocki* (Hexapoda: Diplura): High genetic divergence in a morphologically uniform taxon. Gene. 2006;381:49–61. https://doi.org/10.1016/j.gene.2006.06.009.
100. Clare EL, Kerr KCR, von Königslöw TE, Wilson JJ, Hebert PDN. Diagnosing Mitochondrial DNA Diversity: Applications of a Sentinel Gene Approach. J Mol Evol. 2008;66(4):362–7. https://doi.org/10.1007/s00239-008-9088-2.
101. Chen C, Li Q, Fu R, Wang J, Xiong C, Fan Z, Hu R, Zhang H, Lu D. Characterization of the mitochondrial genome of the pathogenic fungus *Scytalidium auriculariicola* (Leotiomycetes) and insights into its phylogenetics. Sci Rep. 2019;9:17447. https://doi.org/10.1038/s41598-019-53941-5.
102. Zhang Y, Yang G, Fang M, Deng C, Zhang KQ, Yu Z, Xu J. Comparative analyses of mitochondrial genomes provide evolutionary insights into nematode-trapping fungi. Front Microbiol. 2020;11:617. https://doi.org/10.3389/fmicb.2020.00617.
103. Drummond AJ, Ho SYW, Phillips MJ, Rambaut A. Relaxed phylogenetics and dating with confidence. PLoS Biolo. 2006;4(5): e88. https://doi.org/10.1371/journal.pbio.0040088.
104. Ho SY, Duchêne S. Molecular-clock methods for estimating evolutionary rates and timescales. Mol Ecol. 2014;23(24):5947–65. https://doi.org/10.1111/mec.12953.
105. Brown RP, Yang Z. Rate variation and estimation of divergence times using strict and relaxed clocks. BMC Ecol Evol. 2011;11:271. https://doi.org/10.1186/1471-2148-11-271.
106. Asem A, Eimanifar A, Van Stappen G, Sun SC. The impact of one-decade ecological disturbance on genetic changes: a study on the brine shrimp *Artemia urmiana* from Urmia Lake. Iran PeerJ. 2019;7: e7190. https://doi.org/10.7717/peerj.7190.
107. Asem A, Schuster R, Eimanifar A, Lu H, Liu C, Wu X, Yao L, Meng X, Li W, Wang P. Impact of colonization of an invasive species on genetic differentiation in new environments: A study on American *Artemia franciscana* (Crustacea: Anostraca) in the United Arab Emirates. J Ocean Univ China. 2021;20:911–20. https://doi.org/10.1007/s11802-021-4675-6.
108. Cai Y. New *Artemia* sibling species from PR China. Artemia Newslett. 1989;11:40–1.
109. Mura G, Del Caldo L, Fanfani A. Sibling species of *Artemia*: a light and electron microscopic survey on the morphology of frontal knobs Part I. J Crustac Biol. 1989;9(3):414–9. https://doi.org/10.1163/193724089X00386.
110. Mura G, Fanfani A, Del Caldo L. Sibling species of *Artemia*: a light and electron microscopic survey of the morphology of the frontal knobs Part II. J Crustac Biol. 1989;9(3):420–4. https://doi.org/10.1163/193724089X00395.
111. Barigozzi C. *Artemia*: a survey of its significance in genetic problems. In: Dobzhansky T, Hecht MK, Steere WC, editors. Evolutionary Biology. Boston: Springer; 1974. p. 221–52.
112. Abreu-Grobois FA, Beardmore JA. Genetic differentiation of the brine shrimp *Artemia*. In: Barigozzi C, editor. Mechanisms of Speciation. New York: Alan R. Liss; 1982. p. 345–76.
113. Asem A, Rastegar-Pouyani N, De los Rios P. The genus *Artemia* Leach, 1819 (Crustacea: Branchiopoda): true and false taxonomical descriptions. Lat Am J. Aquat Res. 2010;38(3):501–506. https://doi.org/10.3856/vol38-issue3-fulltext-14.
114. Mayr E. Systematics and the Origin of Species. New York: Columbia University Press; 1942.
115. Mayr E. Animal Species and Evolution. Cambridge: The Belknap press; 1963.
116. Asem A, Gajardo G, Hontoria F, Yang C, Shen C, Rastegar-Pouyani N, Padhye SM, Sorgeloos P. The species problem in *Artemia* Leach, 1819 (Crustacea: Anostraca), a genus with sexual species and obligate parthenogenetic lineages. Zool J Linn Soc. 2024;202:zlad192. https://doi.org/10.1093/zoolinnean/zlad192.
117. Sainz-Escudero L, López-Estrada EK, Rodríguez-Flores PC, García-París M. Settling taxonomic and nomenclatural problems in brine shrimps, *Artemia* (Crustacea: Branchiopoda: Anostraca), by integrating mitogenomics, marker discordances and nomenclature rules. PeerJ. 2021;9: e10865. https://doi.org/10.7717/peerj.10865.
118. Li WJ, Guo Y, Sun SC. Population genetics of *Artemia urmiana* species complex (Crustacea, Anostraca): A group with asymmetrical dispersal and gene flow mediated by migratory waterfowl. Gene. 2024;894: 147957. https://doi.org/10.1016/j.gene.2023.147957.
119. Mayr E, Ashlock PK. Principles of Systemsatic Zoology. New York: McGraw-Hill; 1991.
120. Aguilar A, Maeda-Martinez AM, Murugan G, Obregon-Barboza H, Rogers DC, McClintock K, Krumm JL. High intraspecific genetic divergence in the versatile fairy shrimp *Branchinecta lindahli* with a comment on cryptic species in the genus *Branchinecta* (Crustacea: Anostraca). Hydrobiologia. 2017;801(1):59–69. https://doi.org/10.1007/s10750-017-3283-3.
121. Bellec L, Debruyne R, Utge J, Rabet N. The first complete mitochondrial genome of *Limnadia lenticularis* (Branchiopoda, Spinicaudata), with new insights on its phylogeography and on the taxonomy of the genus. Hydrobiologia. 2019;826(1):145–58. https://doi.org/10.1007/s10750-018-3724-7.
122. Xu S, Han B, Martinez A, Schwentner M, Fontaneto D, Dumont HJ, Kotov AA. Mitogenomics of Cladocera (Branchiopoda): Marked gene order rearrangements and independent predation roots. Mol Phylogenet Evol. 2021;164: 107275. https://doi.org/10.1016/j.ympev.2021.107275.
123. Sun X, Cheng J. Comparative mitogenomic analyses and new insights into the phylogeny of Thamnocephalidae (Branchiopoda: Anostraca). Genes. 2022;13(10):1765. https://doi.org/10.3390/genes13101765.
124. Bowen ST. The genetics of *Artemia salina*. IV. Hybridization of wild populations with mutant stocks. Biol Bull. 1964;126(3):333–344. https://doi.org/10.2307/1539304.
125. Naganawa H, Mura G. Two new cryptic species of *Artemia* (Branchiopoda, Anostraca) from Mongolia and the possibility of invasion and disturbance by the aquaculture industry in East Asia. Crustaceana. 2017;90(14):1679–98. https://doi.org/10.1163/15685403-00003744.
126. Gomes N, Antunes C, Costa DA. Insights into the Migration Routes and Historical Dispersion of Species Surviving the Messinian Crisis: The Case of *Patella ulyssiponensis* and Epizoic Rhodolith *Lithophyllum hibernicum*. Hydrobiology. 2022;1(1):10–38. https://doi.org/10.3390/hydrobiology1010003.
127. Eimanifar A, Asem A, Djamali M, Wink M. A note on the biogeographical origin of the brine shrimp *Artemia urmiana* Günther, 1899 from Urmia Lake, Iran. Zootaxa. 2016;4097(2):294–300. https://doi.org/10.11646/zootaxa.4097.2.12.

Publisher's Note